C.P. No. 786

C.P. No. 786

MINISTRY OF AVIATION

AERONAUTICAL RESEARCH COUNCIL

CURRENT PAPERS

Effects of Varied Loading Paths on Fatigue Endurances

Part I - Some load fatigue properties of Nimonic 90 at Elevated Temperatures

By

G.P. Tilly

LONDON: HER MAJESTY'S STATIONERY OFFICE

1965

NINE SHILLINGS NET

U.D.C. No. 539.431:669.245

C.P. No.786

December, 1963

Effects of varied loading paths on fatigue endurances

Part I - Some load fatigue properties of Nimonic 90 at elevated temperatures

- by -

G. P. Tilly

SUMMARY

The load fatigue properties of Nimonic 90 have been examined over the nominal speed range of 7 c/hr to 8000 c/min at temperatures between 20°C and 900°C under repeated tension and push/pull test conditions.

It was shown that an increase in test frequency resulted in longer lives to failure at the higher temperatures. Push/pull loading was more severe than repeated tension loading at low temperatures, but became less severe at the higher temperature. An increase in testing temperature increased the incidence of intercrystalline failure whilst increase in test frequency decreased it.

Replaces N.G.T.E. Memo. No. M.373 - A.R.C.25 880.

CONTENTS

TABLES

APPENDICES

ILLUSTRATIONS

1.0 Introduction

It is perhaps surprising that after a century of testing and awareness of fatigue problems, the basic mechanisms and behaviour are still imperfectly understood. Fatigue problems met in service are usually treated as special cases and can rarely be solved by recourse to the conventional tests that are made in most laboratories. The fatigue loading that occurs in gas turbine components produces a complex stress system with an amplitude that varies during service. The information available on variable loading paths is meagre compared with that on an unchanged history and it is difficult to predict a service life from the simple test data most readily available. This problem is also met in complex stress systems where designers often find that the data is unavailable in the required form e.g., in the case of turbine disc designs where biaxial data are required. Here again, it is difficult if not meaningless to apply the uniaxial data and the best that can be done is to design from experience and give a reasonable safety factor.

This paper is concerned with the first phase of an investigation on variable fatigue loading paths. It is intended to cover a wide range of fatigue conditions prior to attempting to fit some of these together into a variable history. The ultimate aim of this type of approach is to be able to predict service lives from a minimum number of simplified tests such as uniaxial fatigue, short time tensile fracture and creep.

1.1 Fatigue loading of the gas turbine

The temperature range over which a typical gas turbine operates is from ambient to around 850°C with occasional peak conditions up to 1000°C. Resonant vibrations in blades set up bending fatigue stresses at frequencies of the order of 6000 c/min with variations above and below this figure. There are also transient thermal stresses imposed by the heating and cooling of a civil aircraft engine during flight at rates of 1 or 2 c/hr depending on how the throttle is operated and on the duration of flight. The repetition of such transient thermal stresses can cause failure by thermal fatigue. Military aircraft engines might be expected to undergo a more severe form of thermal fatigue during operations involving variations in power output with a consequent increase in the frequency and number of applied cycles through rapid changes in speed and altitude. This form of loading can be simulated by the temperature cycling of a test-piece gripped between two rigid holders or alternatively, by a test-piece raised to the upper temperature and cycled between the relevant strain limits.

2.0 Low cycle fatigue

The simplifications of the thermal fatigue problem clearly leave a number of questions in abeyance, for example, the thermal shock condition of a turbine blade is not truly one of constant strain because the temperature gradients vary according to the particular flight operation and the applied cycles might be close to constant stress or even constant load. Figure 1 illustrates these three classes of fatigue and shows the inter-dependencies of strain, load, stress and time. (In order to simplify the diagram the cycles have been drawn as repeated tensile loading with a saw-tooth load-time application in preference to the more common equal and opposite push/pull with a sinusoidal loading path). In the case of Figure 1.1, the cycles are between constant strain limits and as

the test progresses, the maximum applied load is decreased and the minimum is made compressive in order to maintain the specimen between the strain limits and correct its "cyclic creep"[1]. In Figure 1.2, the cycles have constant load limits, and as the material is progressively strained the cross-section decreases and the true stress is increased. With constant stress cycles (Figure 1.3), the maximum load is progressively decreased to maintain the true stress constant, and it has been found that the cumulative strain obeys creep/time relations similar to those found in static creep tests, although the final fracture strains usually exceed those in comparable static tests[2,3,4].

In addition to these features of cycle control there is also the problem of complex loading[5]. The bulk of fatigue data is based on uniaxial conditions whilst a number of investigations have been made with reverse bending (a mild form of biaxial stressing) either to avoid the problem of compressive buckling during high stress push/pull tests or to simulate a particular service condition. It can be argued that the former gives basic data from which fundamental fatigue mechanisms can be investigated although it is rarely encountered in engineering structures, whilst the latter, though having a more practical application, suffers from the drawback that neither stress nor strain can be recorded meaningfully. A number of combined stress tests have been devised (e.g., tension and torsion, tension and bending) and the data can be used for specialised conditions. Unfortunately the analysis of complex stress systems can be rather tedious and the fatigue data are even more difficult to interpret and predict than for the uniaxial case.

Most of the early investigations were made at high frequencies and at stresses within the elastic region of the material (since the elastic range is itself dependent on the rate of loading). The cycles to failure usually exceeded 10^4. The problem of low cycle fatigue* was encountered in recent years in fatigue tests at applied frequencies of around 10 c/min and endurances of less than 10^4 cycles. Under these conditions the elastic limit was exceeded and an appreciable degree of plastic strain was produced. Thus the type of cycle chosen became important whereas in the high frequency "quasi-elastic" region the form of the cycle is unchanged because stress, strain and load amplitudes remain constant. Strain cycling fatigue tests have been conducted on a variety of materials and it has been shown[6] that a logarithmic plot of plastic strain range against the number of cycles to failure gives a straight line of slope close to $-\frac{1}{2}$. Tests at elevated temperatures indicate an increase in slope although no laws for this temperature dependence have been suggested. Strain controlled cycles have received great attention in recent years on the grounds that they have an apparently closer correspondence with practical applications whilst load cycles have been given less attention and stress cycles have been almost totally neglected. Many of the established features of conventional fatigue do not necessarily apply to the low cycle region. A particular example of this is the room temperature speed effect which has been previously considered to be either very small or negligible over ranges of 500 to 10,000 c/min[7 to 10]. This is not necessarily true of low cycle fatigue.

*Low cycle fatigue may be defined as fatigue failure in less than 10^4 cycles. It has been alternatively referred to as high stress fatigue.

2.1 Elevated temperature effects

There have been numerous investigations on the effect of temperature on the mechanical properties of materials. In general, the elastic limit, ultimate tensile strength, hardness, fatigue and creep strength decrease whilst ductility increases with increased temperature. Sometimes there are irregularities in these relations and the commercial high temperature alloys used in gas turbines mostly exhibit abnormal regions (e.g., the ductility trough in Nimonic 90) usually associated with ageing effects. With increase in temperature the mode of deformation changes from one of transcrystalline slip at low temperature to intercrystalline movements and precipitation controlled mechanisms at the higher temperatures. In the fatigue loading of engineering materials, fractures are predominantly transcyrstalline at the lower temperatures and the number of repetitions to failure are generally constant for varied cycle rates. Fractures are mostly intercrystalline at high temperatures and for varied frequencies it is the time to failure that is virtually constant.

Eckel[11] has shown that for the repeated bending fatigue of lead at room temperature the time to failure is related to the applied cycle frequency by an expression of the form:

$$tf^m = b$$

t time to failure
f applied frequency
m,b constants

In drawing attention to this relation Allen and Forrest[12] pointed out that if m is made equal to 1 then the expression covers the case of low temperature type fatigue of engineering materials where it is the number of repetitions of a given applied stress that cause failure. If m = 0, the time to failure for a given applied stress becomes constant and the behaviour is that expected for high temperature fatigue, where the duration of stress rather than the number of repetitions causes damage. This approach is a simplification of the behaviour of high temperature alloys.

Finally there is the effect of tensile mean stress on hot fatigue behaviour (Figure 2.2). It is generally accepted[13] that increasing tensile mean stress increases the tendency of the material to intercrystalline failure. Conversely, decreasing tensile mean stress increases the tendency to transcrystalline failure.

3.0 Experimental programme

The experimental programme was aimed at producing a field of results for Nimonic 90 over a wide range of fatigue variables i.e., temperature, applied frequency, stress ratio, and cycle control. The first three were treated in this programme and cycle control will be considered at a later date. The tests were conducted at room temperature, 600, 700, 800 and 900°C at frequencies of around 7 c/hr, 10 c/min and 8000 c/min, and stress ratios of -1 and 0. Thus, thirty conditions were

covered in all. The tests were made at different stress levels such that stress-time curves could be plotted for durations ranging from a few minutes to 100 hr to failure.

3.1 Experimental technique

The fatigue tests were made on an Amsler Vibrophore machine under closely similar experimental conditions to those of a previous investigation[14]. There were two ranges of frequency available; a high frequency range of 4000 to 15,000 c/min and an equivalent low frequency range of 7 c/hr to 10 c/min. The high frequency tests were made with a sinusoidal load-time characteristic since the operation was on a resonant principle such that the frequency remained substantially constant over the range of loads available. The low frequency tests were made with a special loading adaptation described in Appendix II. The number of cycles applied per minute was dependent upon the size of the specimen and the desired stress range. Fortunately the frequency variation through different specimen cross-sections was very small compared with the testing range and was unlikely to be significant.

Fatigue loading was commenced as soon as the temperature had settled down to a steady state. The required load amplitude was usually attained after two or three cycles for 10 c/min tests, and during the first cycle for the 7 c/hr tests. Hysteresis heating during the first few minutes of these tests, though less severe than for the high frequency (4000 to 15,000 c/min) tests, was adjusted by the technique of starting the test slightly below temperature and continuing to correct during the first half hour. Most tests were restricted to one week duration in order to complete the experimental programme and tests on specimens unbroken after this time were shut down.

The general size and shape of the test-pieces has also been described previously[14], but some small departures were made from the original geometry. The sizes of the test-sections were selected by reference to the required stresses since the total applied loads were limited to the 2 ton or 10 ton ranges available on the testing machine.

The test-section diameters were selected to give cross-sections of $\frac{1}{65}$, $\frac{1}{30}$, $\frac{1}{20}$ and $\frac{1}{10}$ square inches for convenience of the rough stress calculations. All the elevated temperature test-pieces had parallel gauge lengths of 0.25 in. In general, specimens with $\frac{3}{8}$ in. threaded ends were used at room temperature, $\frac{1}{2}$ in. threaded ends were used at 600°C and 700°C, and $\frac{5}{8}$ in. ends were used at 800°C and 900°C. These small variations in specimen size and geometry did not appear to have any significant effect over the range of test conditions used.

3.2 Material

The tests were made on two heats of 'research quality' Nimonic 90 supplied as $\frac{3}{4}$ in. diameter forged bars in the fully heat treated condition (solution treated at 1080°C for 8 hr and aged 700°C for 16 hr). The chemical analyses of the heats are given below:

Element	Percentage Composition	
	N.G.T.E. Code	
	A.771	C.229
C	0.06	0.06
Si	0.52	0.76
Cu	-	0.06
Fe	0.7	0.85
Mn	0.05	0.08
Cr	18.3	19.8
Ti	2.73	2.53
Aℓ	1.67	1.43
Co	17.5	16.8
Ni	balance	

The results of a number of tests designed to correlate the behaviour of both heats for a range of testing conditions between 600 and 900°C are described in Appendix II.

4.0 Results

Repeated tension and push/pull fatigue tests were conducted over the temperature range of 20°C to 900°C at mean frequencies of 7 c/hr, 10 c/min and 8000 c/min. The results were plotted in the form of log stress/log time (S/t) graphs (Figures 4 to 13) and the best straight lines or curves were drawn through the points. In Figures 14 to 18, the stresses to give 10 hr and 100 hr lives were plotted semi-logarithmically against temperature.

4.1 Repeated tension tests (R = 0)

It is clear that variations in the applied frequency did not have a simple progressive effect over a range of temperatures. In general the material was weakest under high frequency fatigue (8000 c/min) test conditions at temperatures of 700°C and below but underwent a reversal and became stronger above this temperature.

It can be seen from Figure 14 that the 10 hr fracture stresses in the 7 c/hr and 10 c/min tests were similar at all temperatures except 700°C. Figure 8 showed that the slowest frequency (7 c/hr) tests gave lives greater than the 8000 c/min but less than the 10 c/min tests at 700°C i.e., the order of strength was 10 c/min, 7 c/hr, 8000 c/min - for tests with material from both A.771 and C.229 heats. At 900°C the order of merit was 8000 c/min, 10 c/min and 7 c/hr (a reversal of the room temperature order) and the 10 c/min S/t curve had a pronounced irregularity at ~6 hr to failure (Figure 8). In Figure 14, the 8000 c/min 10 hr cross-plot exhibited maximum strength at 700°C. Tests on both

heats showed that the fatigue strength was apparently greater at 700°C than 600°C.

The slopes (K) of the S/t curves were of course negative since decreasing stress allowed a longer life to failure. The value of K rose with increasing temperature and decreasing applied stress. There was not necessarily any significance in the quantitative values of K however, since the stresses in question were nominal and no correction was made to true stress. There was no tendency for the curves to flatten out to a fatigue limit over the range of stresses applied.

The effect of applied frequency can be expressed in terms of the power m taken from the Eckel expression (Appendix III) on the assumption that t is directly proportional to f^m for Nimonic 90. (The efficacy of the expression appeared to be dependent upon the testing conditions, and the value of m was a qualitative rather than exact description of the behaviour of this material.) A stress level was selected at each temperature such that the times to failure for the three test frequencies could be derived from the S/t curves and log t was plotted against log f. As the log t/log f relations were almost linear the approximate mean slopes (m) were evaluated and plotted against temperature (Figure 19). At room temperature m was 0.83 and it was clear that the number of cycles to failure was nearly independent of frequency. The small frequency effect indicated that the higher frequencies gave slightly longer lives (as measured by cycles to failure). The value of m decreased with increasing temperature, becoming 0 at between 700 and 800°C (time to failure independent of the applied frequency) and increasingly negative at 800 and 900°C i.e., higher frequencies gave longer lives to failure as measured by either cycles or time.

4.2 Push/pull tests (R = -1)

The high frequency push/pull fatigue tests, compared with the low frequency push/pull type, gave shorter lives at 20°C to 800°C and longer lives at 900°C with an anomalous cross-over similar to that observed in the repeated tension tests at 700°C where the order of strength was 10 c/min, 7 c/hr and 8000 c/minute.

The frequency effect for the push/pull test data was expressed in terms of the power m, and as for the repeated tension tests, m decreased with increasing temperature (from 1.13 at 20°C to 0.1 at 900°C), but did not become negative at the higher temperatures.

4.3 Push/pull versus repeated tension tests

The room temperature tests illustrated that push/pull fatigue was more severe than repeated tension when considered in terms of the maximum applied stress. There was an inversion of this effect at the higher temperatures. The 7 c/hr push/pull tests indicated an increased strength as compared with repeated tension tests above 700°C, and the 10 c/min push/pull tests became stronger at 900°C. The 8000 c/min frequency test specimens remained weaker in push/pull loading over the whole temperature range.

In Figure 19 it can be seen that for push/pull fatigue, the frequency factor m was higher than in the case of repeated tension, particularly at the higher temperatures. At room temperature m was close to 1 for both cases (failure determined by the number of repetitions) whilst at 800°C $m_{R=-1}$ was 0.65 (strongly cycle dependent) and $m_{R=0}$ was -0.065

(almost completely time dependent). The inference was that fatigue behaviour under push/pull test conditions remained more cycle dependent at higher temperatures than that under conditions of repeated tension.

The slopes of the S/t curves for some push/pull tests tended to become zero at lower stresses and were similar to those of the fatigue curves for materials with an endurance limit. The repeated tension tests showed no such tendency and were close to either straight lines or creep type curves with increasing K at decreasing stress levels.

The 100 hr static creep stresses[20] were also plotted in Figures 17 and 18 in order to compare static and fatigue loading strengths. (The values of the static creep stresses plotted in Figures 17 and 18 were pessimistic, but appeared to form a useful basis for comparison of the respective type of loading.) It was clear that the material was more resistant to interrupted loading than static loading at the higher temperatures, and that for a given frequency there was a changeover temperature below which it was stronger in creep (and above which it was stronger in fatigue). For the 8000 c/min tests this transition temperature was ~670°C for repeated tension and ~750°C for push/pull tests.

5.0 Metallographic examination

Two forms of metallographic examination were made on the fractured specimen; macroscopic examination of the fracture surfaces and microscopic examination at magnifications up to 500X of sections taken perpendicular to the fracture. The fracture types were classified from the macroscopic observations and verified as either intercrystalline or transcrystalline from the microscopic sections of which typical examples are given in Figures 20.2 and 20.3. There were a number of variations on these two types and several in the transition region had fatigue-type initiations followed by creep-type fracture. Table I shows the type of fracture found for each group of tests and it can be seen that the incidence of creep-type fractures was greatest in the low frequency and high stress ratio tests.

Microscopic examination showed that the fractures with a macroscopic creep appearance were intercrystalline and that many of the fatigue and shear-type failures exhibited a small number of intercrystalline cracks although failure was predominantly by a transcrystalline mode. The general trend was for failure at the lower temperatures to be ductile with either a cup-and-cone form or 45° shear planes. An increase in testing frequency at the lower temperatures reduced the fracture ductility and increased the incidence of 90° and multiplanar fractures. An increase in temperature reduced the fracture ductility and introduced some creep-type areas on the 45° planes. The very high temperature failures were entirely on 90° planes and had a brittle appearance inasmuch as there was little or no necking and the fracture ductilities were of the order of 1 to 5 per cent elongation as compared with 20 per cent at room temperature. Fatigue cracks were confined to the high frequency tests and appeared to initiate some of the 800°C and 900°C failures where the final separation was by a creep-type mode.

Striations associated with fatigue mechanisms[18,19] were observed at 500X magnification (see Figure 20.1) on the fracture facets of the 8000 c/min tests at 20°, 600° and 700°C, in both repeated tension and push/pull tests. The 7 c/hr and 10 c/min tests exhibited isolated regions of striations but they were otherwise absent at these temperatures as well as at 800° and 900°C.

Intergranular cracks that were present in areas adjacent to the fracture in high temperature test specimens were mostly wedge-type (see Figure 20.3). There was no clear-cut evidence of voids or rounded cavities often found adjacent to creep fractures. The low temperature deformation mechanisms remained operative for most of the testing range since slip markings were still in evidence at 900°C and twinning was still apparent at 700°C. There was negligible evidence of intergranular oxidation and it appeared unlikely that it played an important part in the tests lasting less than 100 hr to failure. The high frequency tests suggested an acceleration in the precipitation of the γ' phase ($Ni_3[Al,Ti]$, the major precipitation-hardening phase in the Nimonic 90 alloy system), but the lower frequency tests showed little or no such effect.

The C.229 material was more uniform in grain size and distribution of precipitates than was the A.771 which showed severe banding and a very irregular grain size. The A.771 material was stronger in fatigue than the C.229 over the ranges of comparison but possibly exhibited a little more scatter in properties. These features may be associated with the variations in microstructure, but there was insufficient evidence to draw any firm conclusion.

6.0 Discussion of results

High temperature constant load amplitude fatigue may be considered in terms of two competing mechanisms; a fatigue mechanism where life is governed by the number of repetitions of load, and a creep mechanism governed by the total time endured. The former mechanism predominates at room temperature where the cycles to failure at varied frequencies are virtually constant, while the latter predominates at elevated temperatures where the time to failure becomes constant. There is a transition region of temperature expressed schematically in Figure 2 where the creep and fatigue curves for an idealised material with no irregularities were plotted against temperature, and cross over at a given value. This transition can be ideally defined as the temperature at which neither the number of cycles nor the duration of loading predominate and the life to failure is determined by both cycles and duration. The transition might be expressed as the temperature at which the frequency factor m is equal to 0.5. The changeover in fracture type could be taken as an alternative definition of transition since the high temperature fractures are mostly intercrystalline and the low temperature fractures are transcrystalline. This fracture changeover is spread over a range of temperature whose mean value does not necessarily coincide with the point where m = 0.5. In many ways it is similar to the brittle/ductile transition in body-centred cubic structures since it is affected by changes in testing conditions such as the rate of loading and nature of the stresses and can be defined in a number of ways.

The cross-plot curves in Figures 14 to 18 are the resultant curves formed from the creep and fatigue contributions and it is clear from the relative spacing of the curves that the differing frequencies and stress ratios affect the relative contribution of the two mechanisms. The failures from the 8000 c/min push/pull tests were all transcrystalline up to 900°C whereas the low speed failures became intercrystalline at 700 to 800°C. An increase in stress ratio from R = -1 to R = 0 also increased the transition temperature as evinced by Figure 19 where values of m are lower for repeated tension than for push/pull tests at the same

temperature and failure ceased to be cycle-dependent at a lower temperature. An increase in testing frequency therefore increases the incidence of cycle-dependent transcrystalline fatigue failures with respect to temperature, and raises the transition. An increase in stress ratio (increasing tensile mean stress) decreases the fatigue incidence and lowers the transition temperature.

It is interesting to note that the room temperature repeated tension fatigue curves show a small speed effect at very high stresses close to the static fracture stress which suggests that even at this temperature the time-dependent mechanism has some effect on the results. The fact that the complementary push/pull tests show no such effect ($m \simeq 1.13$ at room temperature) may be due either to the lower stress ratio increasing the effect of the fatigue component or may be associated with some instability at very high compressive stresses.

It is also of interest to compare the two previous investigations made on similar heats of Nimonic 90 (References 14, 15 and 16). Both reported small frequency effects over limited ranges though neither appeared significant. Stephenson's tests[14] in the range 20 to 900°C all resulted in transcrystalline fractures by virtue of a high testing frequency and low stress ratio whereas Landau, using a high stress ratio and low frequencies, produced time-dependent creep failures. Thus the latter tests were made under conditions such that fractures were to the high temperature side of the transition temperature.

It is clear from the room temperature S/t curves that the frequency effect becomes increasingly important at high stresses where the slope K is very small. The static ultimate tensile strength (U.T.S.) can be related to the fatigue curves at the correct testing speed for room temperature tests[17] and it is evident from the above tests that this is also true at elevated temperatures. There is a very marked reduction in slope at the high stress end of the S/t curve and it is perhaps not surprising that some materials either fracture during the first cycle or else last for some time. In Figure 4 the U.T.S. is related to the fatigue stresses by a region with a very low slope and it appears that failure can only be achieved in this region under favourable testing conditions. This region was absent in the 8000 c/min tests and was less well defined for the 10 c/min tests than for those at 7 c/hour. Other metals and their alloys might have slopes so low as to make it impossible to obtain fractures between the U.T.S. and the steeper region even at very low testing speeds. The 10 c/min curves at 600 to 900°C were all extrapolated through the U.T.S. values determined at that loading rate but showed no sudden change in curvature.

The presence of striations on the fracture surfaces of specimens tested at 20°, 600° and 700°C in both repeated tension and push/pull at 8000 c/min together with isolated regions observed at 7 c/hr and 10 c/min as well as the 800° and 900°C tests is interesting. It appears that the presence of striations indicates failure by a fatigue mechanism, although their absence does not necessarily eliminate this. The failure mechanism of the slow speed tests in the absence of large regions of striations would appear to be by other than conventional fatigue and is almost certainly associated with delayed static fracture[21].

7.0 Conclusions

(i) The changes in fatigue properties of Nimonic 90 with increasing temperature are not a smooth continuous process but vary according to testing conditions and contain some apparent anomalies.

(ii) Low temperature transcrystalline failures may be considered as being basically cycle-dependent and high temperature intercrystalline failures are time-dependent. The transition between transcrystalline and intercrystalline fracture does not necessarily coincide with that between cycle and time-dependent failure.

(iii) Hot fatigue behaviour is affected by both applied frequency and stress ratio. An increase in frequency gives shorter lives at low temperatures but longer lives at high temperatures. Similarly, the lower stress ratio (push/pull) tests give shorter lives than those under repeated tension at room temperature but longer lives at higher temperatures.

(iv) The static U.T.S.'s determined at the correct testing speeds and temperatures lie on the load fatigue curves and it appears that they are related to the S/t curves over the range of conditions tested.

(v) The metallographic examination of fractured specimens showed a continuous changeover in fracture type from transcrystalline shear at the lower temperatures to intercrystalline creep at the high temperatures. An increase in applied frequency at a given temperature increased the tendency to transcrystalline fracture.

ACKNOWLEDGEMENTS

The assistance of Mr. W. Gwenlan who set up the fatigue test-pieces and prepared the specimens for metallographic examination, and Mr. J. E. Northwood who supervised the preparation of metallographic sections is gratefully acknowledged.

NOTATION

U.T.S.	ultimate tensile strength expressed in ton/in^2
R	ratio of minimum to maximum stress in a fatigue cycle (see Figure 2.2)
S	maximum applied stress/cycle
N	number of cycles to failure
t	life to failure in hours
T	testing temperature
K	slope of Log S/Log N and Log S/Log t curves
m	frequency factor
f	applied frequency
b	constant for a given stress

REFERENCES

No.	Author(s)	Title, etc.
1	P.P. Benham	Fatigue of metals caused by a relatively few cycles of high load or strain amplitude Metallurgical Reviews 1958 3 No.11
2	F. H. Vitovec	On dynamic creep with special consideration of strain effects Proc. ASTM, 47, 1947, p.977
3	F. W. DeMonez D. J. Lazan	Dynamic creep and rupture properties of an aluminium alloy under axial static and fatigue stress ASTM 54, 1954, p.769
4	G. P. Tilly P. P Benham	Load cycling in the low endurance range in relation to brittle fracture of mild steel J. of Iron and Steel Inst. 200, 1962, p.216
5	H. J. Gough H. V. Pollard W. J. Clenshaw	Some experiments on the resistance of metals to fatigue under combined stresses ARC R. & M. No.2522, 1951
6	L. F. Coffin	A study of the effects of cyclic thermal stresses on a ductile metal Trans. ASME 76, 1954, p.931
7	S. R. Valluri	Effect of frequency and temperature on fatigue of metals NACA TN 3972 February 1957
8	G. N. Krouse	A high speed fatigue testing machine and some tests of speed effect on endurance limit Proc. ASTM 34, 1934, p.156
9	A. J. McEvily, Jr. E. S. Machlin	The effect of repeated stressing on the behaviour of Lithium Fluoride crystals NASA TR-R-91 1961
10	N. Stephenson	A review of the literature on the effect of frequency on the fatigue properties of metals and alloys NGTE Memorandum No. M.320 June 1958 A.R.C.20 475
11	J. F. Eckel	The influence of frequency on the repeated bended life of acid lead Proc. ASTM 51, 1951, p.745

REFERENCES (cont'd)

No.	Author(s)	Title, etc.
12	P. G. Forrest N. P. Allen	The influence of temperature on the fatigue of metals Proc. Int. Conf. Fatigue of Metals 1956 I. Mech. E - ASTM, p.327
13	A. H. Heleka	Combined creep and fatigue properties Metallurgical Reviews 1962, 7, No. 25
14	N. Stephenson J. E. Northwood R. S. Smith	The effect of alternating stresses at elevated temperatures on structural changes in Nimonic 90 NGTE Memorandum No. M.325, July, 1959
15	C. S. Landau	Low frequency fatigue of Nimonic 90 NGTE Report No. R.243 September, 1960 A.R.C.22 309
16	C. S. Landau	Low frequency fatigue - a rheological approach The Engineer 214, 1962, p.911
17	P. P. Benham H. Ford	Low endurance fatigue of a mild steel and an aluminium alloy J. of Mech. Eng. Science 3, 1961, p.119
18	P. J. E. Forsyth D. A. Ryder	Some results of the examination of aluminium alloy specimens fracture surfaces Metallurgia 63 No. 377, March 1961 p.117
19	C. A. Zappfe C. D. Worden	Fractographic registrations of fatigue Trans. ASME 1951 43, p.958
20		The Nimonic alloys. Design Data Henry Wiggin and Co. Ltd. Fifth edition
21	W. A. Wood	Some basic studies in the fatigue of metals Fracture Conference April 1959 edited by Auerbach et al

TABLE I

Fracture modes at varied testing conditions

Temp. °C	Frequency	Type of fracture* Repeat Tensile R = 0		Push/Pull R = -1	
600	7 c/hr	Creep	(I)	45° Shear	(T)
	10 c/min	Shear	(T)	Mostly shear some creep	(70% T)
	8000 c/min	Fatigue	(T)	Fatigue	(T)
700	7 c/hr	Creep	(I)	Creep at 45°	(I)
	10 c/min	Creep at 45° some shear	(I/T)	Creep and 45° shear	(70% I)
	8000 c/min	50% Fatigue some creep	(Mostly T)	90° low ductility	(T)
800	7 c/hr	Creep 90° low ductility	(I)	Creep	(I)
	10 c/min	Creep 90° low ductility	(I)	Creep 90° low ductility	(I)
	8000 c/min	Fatigue/creep	(I/T)	90° low ductility	(T)
900	7 c/hr	Creep 90° low ductility	(I)	Creep 90° low ductility	(I)
	10 c/min	Creep 90° low ductility	(I)	Creep 90° low ductility	(I)
	8000 c/min	Creep 90° low ductility	(I)	Fatigue	(T)

TABLE I (cont'd)

Table I The fracture modes at varied testing conditions

I = intercrystalline failure
T = transcrystalline failure
} determined by microscopic examination

90°, 45° = the angle between the fracture plane and the direction of loading

* = The fracture types were classified as follows:

Shear — The shear fracture faces were parallel to the maximum shear stress planes (45° to the direction of loading for the uniaxial case), and may be either on one plane or on a multiplicity of planes. The appearance under the microscope was dull and there were no bright facets. There was usually some evidence of distortion caused by the faces having slid over one another during fracture.

Fatigue — The fatigue fractures took place with little or no deformation and showed evidence of growth rings where the fracture had propagated in steps.

Creep — Creep fractures had a characteristic granular appearance under the microscope and exhibited little or no necking.

TABLE II

Constant load fatigue tests on Nimonic 90†

Nominal frequency	Maximum applied stress (ton/in²)	Cycles to failure	Life (hr)	Heat Ref.
Repeat tension tests at room temperature				
7 c/hr	79.5	½	0.417	A.771
	77.5	46	7.1	"
	78.8	202	25.95	"
	78.0	409	53.55	"
	76.8	1272	169.0*	"
10 c/min	80.5	½	0.0055	A.771
	77.0	6547	7.8	"
	69.7	16332	16.45	"
	73.7	12988	13.9	"
	78.7	868	0.95	"
	67.2	25171	24.6	
	65.3	37131	35.2	
8000 c/min	78.2	6×10^3	0.0083	A.771
	74.0	14×10^3	0.0194	"
	60.6	98×10^3	0.15	"
	51.2	529×10^3	1.2	"
	42.2	21831×10^3	69.5	"
	45.0	4516×10^3	9.9	"
Push/Pull Tests at room temperature				
7 c/hr	66.3	128	31.2	A.771
	65.8	180	46.0	"
10 c/min	67.2	82	0.25	A.771
	64.0	339	0.7	"
	59.0	911	1.7	"
	54.3	4665	7.7	"
8000 c/min	29.9	780×10^3	1.7	A.771
	26.8	908×10^3	2.0	"
	22.9	1058×10^3	2.5	"
	20.0	51336×10^3	110.8*	"
	21.5	15454×10^3	36.4	"

*Unbroken

† For other 8000 c/min push/pull tests at 600°C, 700°C, 800°C and 900°C on the A.771 heat see Reference 14.

TABLE II (cont'd)

Repeat tension tests at 600°C

Nominal frequency	Maximum applied stress (ton/in²)	Cycles to failure	Life (hr)	Heat Ref.
7 c/hr	67.3	½	0.125	A.771
	60.0	1280	260.8*	"
	63.0	278	68.3*	"
	64.5	59	10.5	"
	60.2	34	7.05	C.229
10 c/min	68.4	½	0.002	A.771
	64.9	210	0.4	"
	61.4	6709	11.6	"
	58.5	83248	140.6	"
	60.5	92788	164.5*	"
	60.1	769	1.4	C.229
8000 c/min	59.8	16×10^3	0.006	A.771
	55.0	96×10^3	0.50	"
	38.7	390×10^3	0.85	"
	49.5	86×10^3	0.35	"
	35.3	709×10^3	3.6	"
	32.3	3787×10^3	206.1*	"
	33.5	49997×10^3	112.4	C.229
	40.0	981×10^3	2.2	"

Push/Pull tests at 600°C

7 c/hr	38.5	510	143.3*	A.771
	54.0	231	89.0*	"
	61.5	43	15.4	"
	64.5	7	3.0	"
	60.2	6	2.5	C.229
10 c/min	57.0	202	0.75	A.771
	50.0	1193	3.9	"
	45.0	1660	5.0	"
	40.0	8454	22.7	"
	36.4	6514	15.8	C.229
	39.7	3508	8.8	"
8000 c/min	26.0	368×10^3	0.9	C.229

*Unbroken

TABLE II (cont'd)

Repeat tension tests at 700°C

Nominal frequency	Maximum applied stress (ton/in^2)	Cycles to failure	Life (hr)	Heat Ref.
7 c/hr	63.7	½	0.14	A.771
	56.0	13	2.1	"
	47.5	65	10.8	"
	55.5	32	5.8	"
	52.3	254	34.8	"
	49.5	103	13.4	"
	43.9	595	86.3	"
	50.3	26	3.75	C.229
	44.1	48	8.15	"
10 c/min	42.5	72371	88.6*	A.771
	44.5	34791	106.6	"
	48.4	31108	43.3	"
	64.7	½	0.003	"
	56.7	5044	8.2	"
	59.2	692	1.2	"
	40.7	6336	12.7	C.229
	38.7	61204	110.4	"
	51.0	4181	6 2	"
8000 c/min	56.6	16000	0.033	A.771
	40.3	1248×10^3	1.4	"
	45.3	1431×10^3	2.95	"
	43.0	1208×10^3	2.5	"
	36.7	32166×10^3	68.3	"
	39.1	27430×10^3	58.4	"
	40.4	2373×10^3	5.5	C.229

Push/Pull tests at 700°C

7 c/hr	45.8	47	13.2	A.771
	47.5	88	33.5	"
	50.0	40	14.4	"
	55.5	15	6.9	"
	50.2	1½	0.55	C.229
	50.4	7	2.95	"
	44.7	25	9.85	"
10 c/min	50.0	502	1.6	A.771
	45.0	582	1.7	"
	42.0	823	2.3	"
	38.0	1619	4.1	"
	30.4	20999	50.6	"
	34.0	3898	6.4	"
	32.3	2403	4.95	C.229
	40.6	460	1.2	"
8000 c/min	26.9	1525×10^3	3.7	C.229

* Unbroken

TABLE II (cont'd)

Repeat tension tests at 800°C

Nominal frequency	Maximum applied stress (ton/in²)	Cycles to failure	Life (hr)	Heat Ref.
7 c/hr	46.6	½	0.122	C.229
	21.4	473	56.8	"
	32.5	53	8.7	"
	25.5	392	57.7	"
10 c/min	28.8	16725	21.9	C.229
	31.1	6534	9.2	"
	20.6	-	156.8*	"
	25.1	44795	51.1	"
	32.5	1895	2.8	"
	22.8	56839	57.3	"
	21.0	37937	119.1	"
	55.0	½	0.0014	"
8000 c/min	32.5	4569×10^3	15.0	C.229
	28.8	20463×10^3	46.4	"
	24.9	27914×10^3	62.0	"

Push/Pull tests at 800°C

7 c/hr	30.1	76	27.0	C.229
	32.5	15	6.8	"
	32.5	53	8.7	"
	27.7	96	30.8	"
10 c/min	29.8	1084	3.4	C.229
	21.0	60752	141.0*	"
	28.5	1626	4.8	"
	25.0	2376	6.4	"
	24.0	10685	27.2	"
	26.1	3597	9.6	"
	22.0	56728	139.65	"
	23.0	27140	59.3	"
8000 c/min	22.6	170×10^3	0.55	C.229
	22.6	-	0.8	"
	19.6	26428×10^3	60.8	"

*Unbroken

TABLE II (cont'd)

Repeat tension tests at 900°C

Nominal frequency	Maximum applied stress (ton/in²)	Cycles to failure	Life (hr)	Heat Ref.
7 c/hr	10.4	320	31.8	C.229
	14.5	62	9.2	"
	22.6	19	2.0	"
	23.1	½	0.11	"
10 c/min	14.4	6611	9.7	C.229
	15.8	7694	4.4	"
	13.3	14818	16.2	"
	12.0	32507	32.0	"
	10.5	174185	163.1*	"
	11.2	68460	69.0	"
	21.1	410	4.3	"
	22.6	932	0.9	"
	43.2	½	0.0017	"
	42.6	½	0.002	"
8000 c/min	11.9	7868×10^2	160.1	C.229
	15.3	28630	59.3	"
	17.8	10350	23.9	"
	20.2	4645	15.9	"

Push/Pull tests at 900°C

7 c/hr	17.8	59	11.7	C.229
	21.6	6	1.6	"
	15.8	103	18.2	"
	13.5	201	32.9	"
10 c/min	15.8	17251	26.8	C.229
	17.3	13226	22.55	"
	21.1	5210	10.8	"
	13.1	60017	140.4*	"
8000 c/min	16.0	4524×10^3	15.4	C.229
	13.05	20593×10^3	48.1	"

* Unbroken

TABLE III

Frequency factors at varied temperatures

Temperature °C	Push/Pull R = -1		Repeat tension R = 0	
	Frequency factor m	Applied stress (t.s.i.)	Frequency factor m	Applied stress (t.s.i.)
20	1.13	65	0.83	77.5
600	The S/t slopes were too low at 600°C to allow meaningful values of the stress intercepts to be recorded.			
700	0.65	30	0.42	50
800	0.65	25	-0.065	30
900	0.1	17.5	-0.17	20

APPENDIX I

The low speed adaptation to the Amsler Vibrophore

During the high frequency operation of an Amsler Vibrophore (Figure 3) the central cross-head C is locked against the vertical pillar P, and fatigue loading is applied to the test-piece T by a vibrator V at resonant speeds determined by the elasticity of the system. Under normal operating conditions these frequencies are of the order of 4000 to 15,000 c/min.

The slow speed adaptation applies load at frequencies ranging from 7 c/hr to 10 c/min and is basically an electric motor M driving a vertical worm W through a two-speed gearbox G and final reduction gear R. The central cross-head C is unlocked and freed to allow the movement of W to deform a large spring S and apply a load to the specimen that is proportional to this deflection. A differential transformer D is energised by the movement of S and feeds the response into a relay circuit which is controlled to reverse the motor M back and forth. The fatigue cycle can be applied between any two predetermined load limits within the range of the machine. The load-time relation is saw-toothed by virtue of the linear spring movement. During high stress tests the deformation or creep of the test-piece causes the motor to do more work deforming the spring but does not change the reversing loads as the spring deformation is independent of the specimen size. The cycles then are of the constant load type (Figure 1.2) and the frequency is dependent upon the applied stress range and the size of the specimen.

An additional compression cross-head guide O was added later to restrain the loading column in the horizontal plane and ensure that the compressive loading is axial and that the specimen cannot buckle at high stresses under first order loads (Figures 3.2 and 3.3) that are operative in cases where the loading is truly axial. The second order buckling takes place under very high axial loads.

APPENDIX II

Correlation of the A.771 and C.229 heats of Nimonic 90

In a previous investigation reported in 1959 (Reference 14) a Nimonic 90 heat with the code A.771 had been used exclusively, and at the beginning of the current investigation there remained 70 untested specimens, together with 57 specimens machined from a second heat (C.229) with enough of that material to manufacture a further 42.

In order to use the 127 specimens as well as the data of the 168 reported tests, a number of experiments were duplicated for the two heats over a variety of conditions. The correlations were made by duplicating 1, 2 or 3 of the A.771 tests at each condition with C.229 material at stresses aimed to give around 10 hr to failure. Thus tests were made with C.229 material for all 24 conditions with comprehensive coverage by A.771 for all conditions at 600 and 700°C and for the high frequency push/pull tests at 800 and 900°C.

The duplicate tests had the merit of correlating the two heats and enabling a larger number of conditions to be covered than could be done with either one alone, and gave additional experimental support to the abnormal trends in behaviour (referred to in Sections 3.1 and 3.2). It appeared that the C.229 heat was inherently weaker than the A.771 over the ranges of speed, temperature and stress ratio tested. If parallel curves were drawn through the duplicate tests it seemed that the separation was similar to that expected by a change in testing temperature rather than stress or time. A simple analysis of the displacements of respective curves suggested that the C.229 could be considered to be between 50 and 100°C weaker than the A.771. This temperature difference compares with variations in the order of only 10°C for the cast to cast differences measured by creep tests.

The high speed (8000 c/min) repeat tension tests at 40 t.s.i. for 600 and 700°C on the A.771 heat suggested that for a range of lives up to 100 hr the material was stronger at 700°C than at 600°C though the test points were rather scattered. Duplicate tests on the C.229 heat at 40 t.s.i. supported this observation with lives of 2.2 and 5.5 hr at the respective temperatures. Duplicate C.229 tests also verified the repeat tensile 'reverse speed effect' at 700°C, referred to in Section 4.1, and it was shown that both melts were strongest (longer lives for a given applied stress) at the faster applied frequency.

APPENDIX III

The frequency factor

Eckel[11] showed that the room temperature repeated bending fatigue of lead at varying applied frequencies could be described by the equation:

$$\text{Log } t = \text{Log } b - m \text{ Log } f$$

In this paper the expression has been rewritten in the form:

$$tf^m = b$$

where b is a constant for a given value of the maximum cyclic stress. The similarity in behaviour between lead at room temperature and Nimonic 90 at elevated temperature has suggested a similar treatment of the Nimonic 90 data. Plots of Log t against Log f did indeed give points reasonably close to straight lines for the three applied frequencies. It was necessary to take a different value of applied stress at each temperature since the strength decreased with temperature and it was impossible to take one stress value for the whole series. The stresses (Table III) were the values that gave maximum time intercepts of 100 hr on the S/t curves at each temperature. Clearly, stress and temperature also affect the behaviour and a more general and meaningful form of the equation is:

$$tf^{\phi(S,T)} = b$$

The value of the slope (m) may be termed the frequency factor or exponent since it appears to be a measure of the effect of frequency on the life to fracture and can be used to describe time or cycle-dependent behaviour. For m to be independent of applied stress, it is necessary for the respective Log S/Log t curves at a given temperature to be parallel. This was not true of the tests however, and there was a tendency for some of the curves to converge with increased stress such that the values of m decreased e.g., the data of Figure 4. The equation is only an approximate description of the behaviour, and the numerical values of m indicate trends rather than exact behaviour.

D 31148/1/Wt.60 K.4 2/65 R/CL

FIG.1.

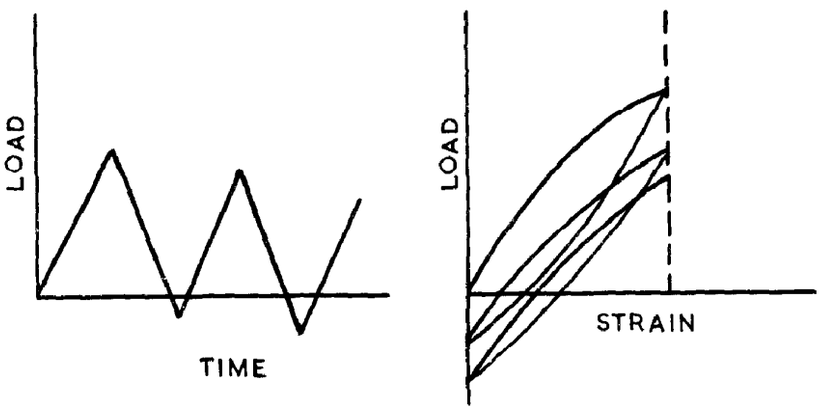

1.1 CONSTANT STRAIN

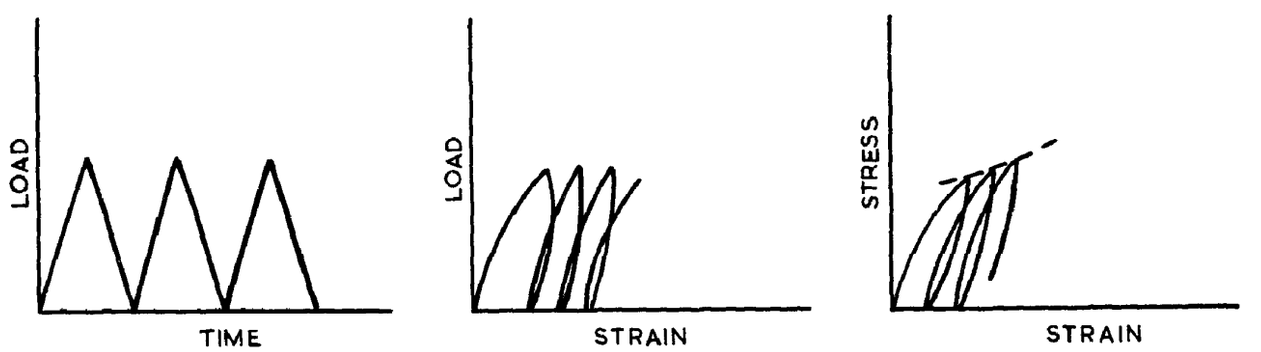

1.2 CONSTANT LOAD

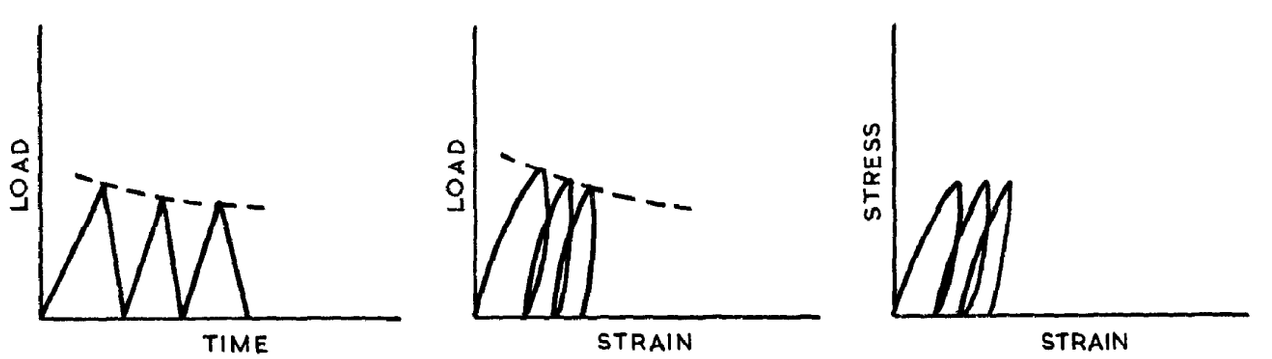

1.3 CONSTANT STRESS

THE BEHAVIOUR OF STRAIN, LOAD AND STRESS CYCLES

FIG. 2.

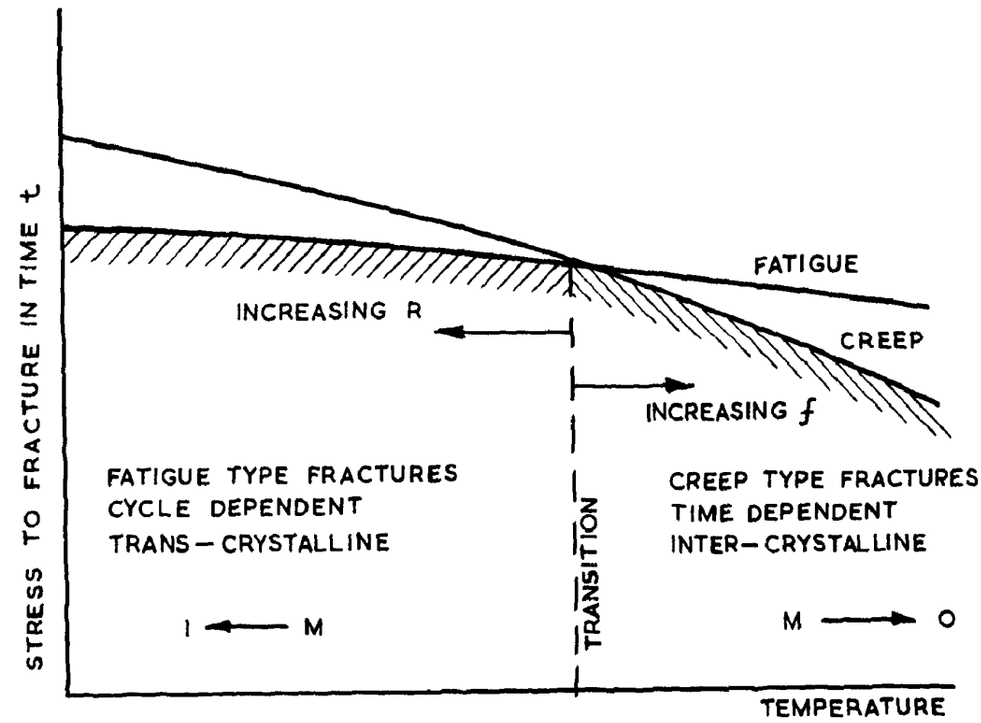

2.1 EFFECTS OF TEMPERATURE ON FRACTURE STRENGTH

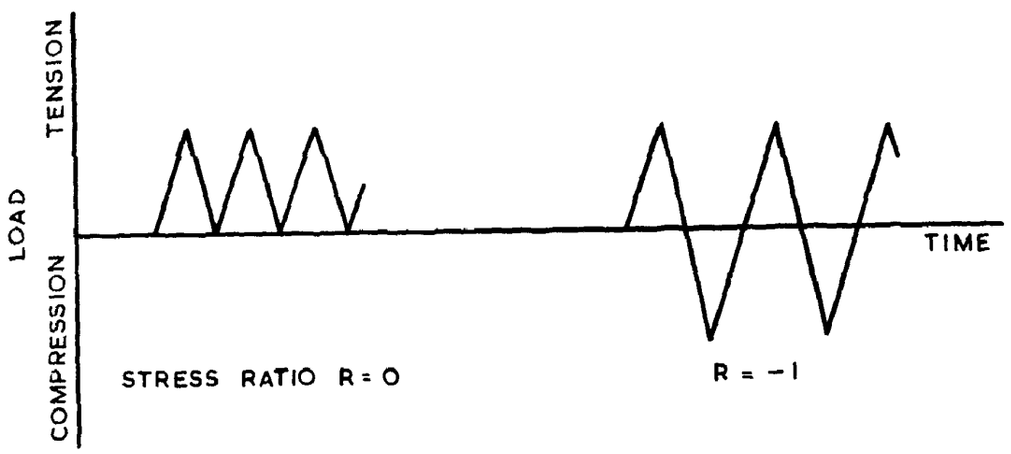

2.2 REPEAT TENSION AND PUSH/PULL FATIGUE CYCLES

FIG. 3.

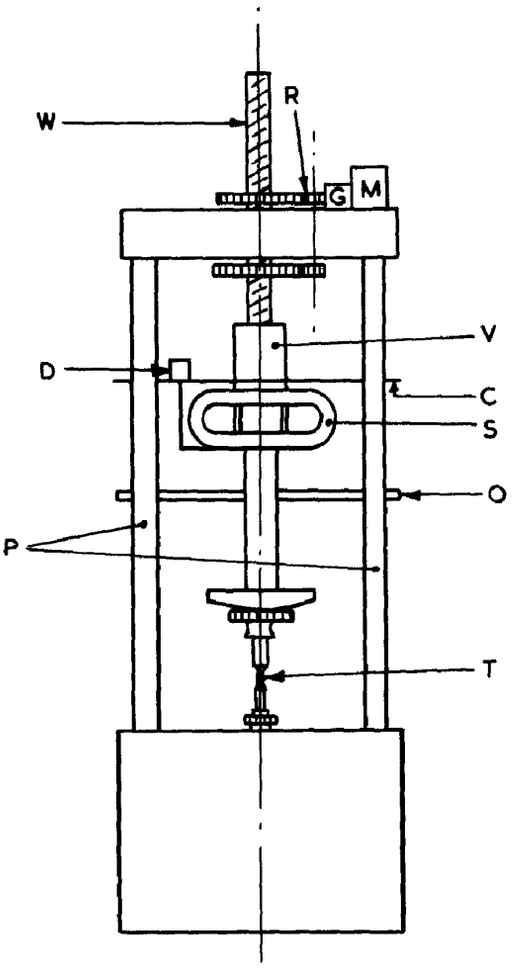

W WORM DRIVE
R REDUCTION GEAR
G TWO SPEED GEAR BOX
M MOTOR
V VIBRATOR
C CROSS-HEAD
S LOAD SPRING
P VERTICAL PILLAR
D DIFFERENTIAL TRANSFORMER
T TEST PIECE
O COMPRESSION CROSS-HEAD GUIDE

3.1 10 TON AMSLER VIBROPHORE WITH SLOW SPEED ATTACHMENT

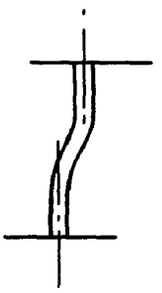

3.2 FIRST ORDER BUCKLING DUE TO NON-AXIAL APPLICATION OF LOAD

3.3 SECOND ORDER BUCKLING OF A SLENDER SPECIMEN

FIG. 4.

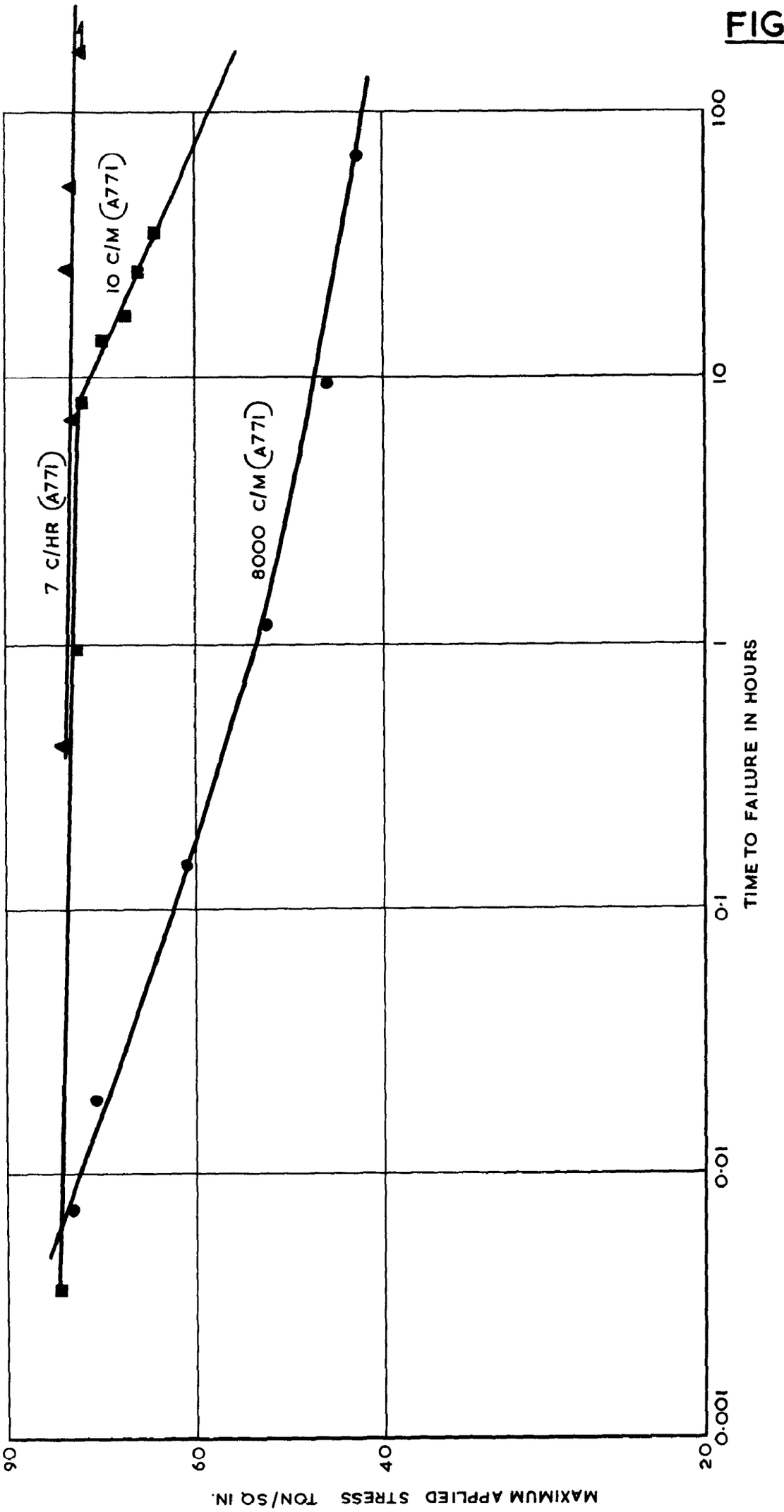

REPEAT TENSION AT ROOM TEMPERATURE

REPEAT TENSION AT 600°C

FIG.5.

FIG. 6.

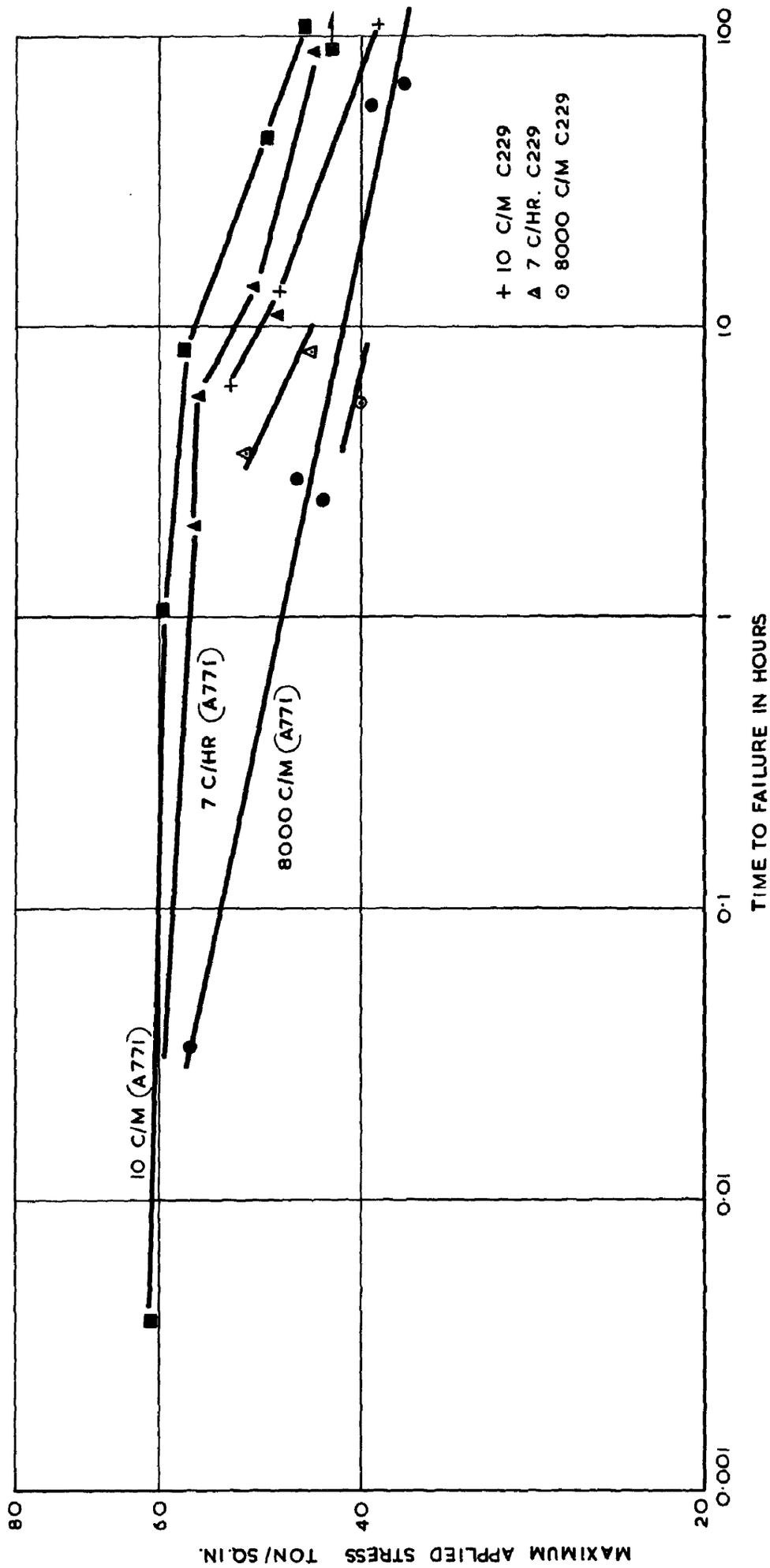

REPEAT TENSION AT 700°C

FIG. 7.

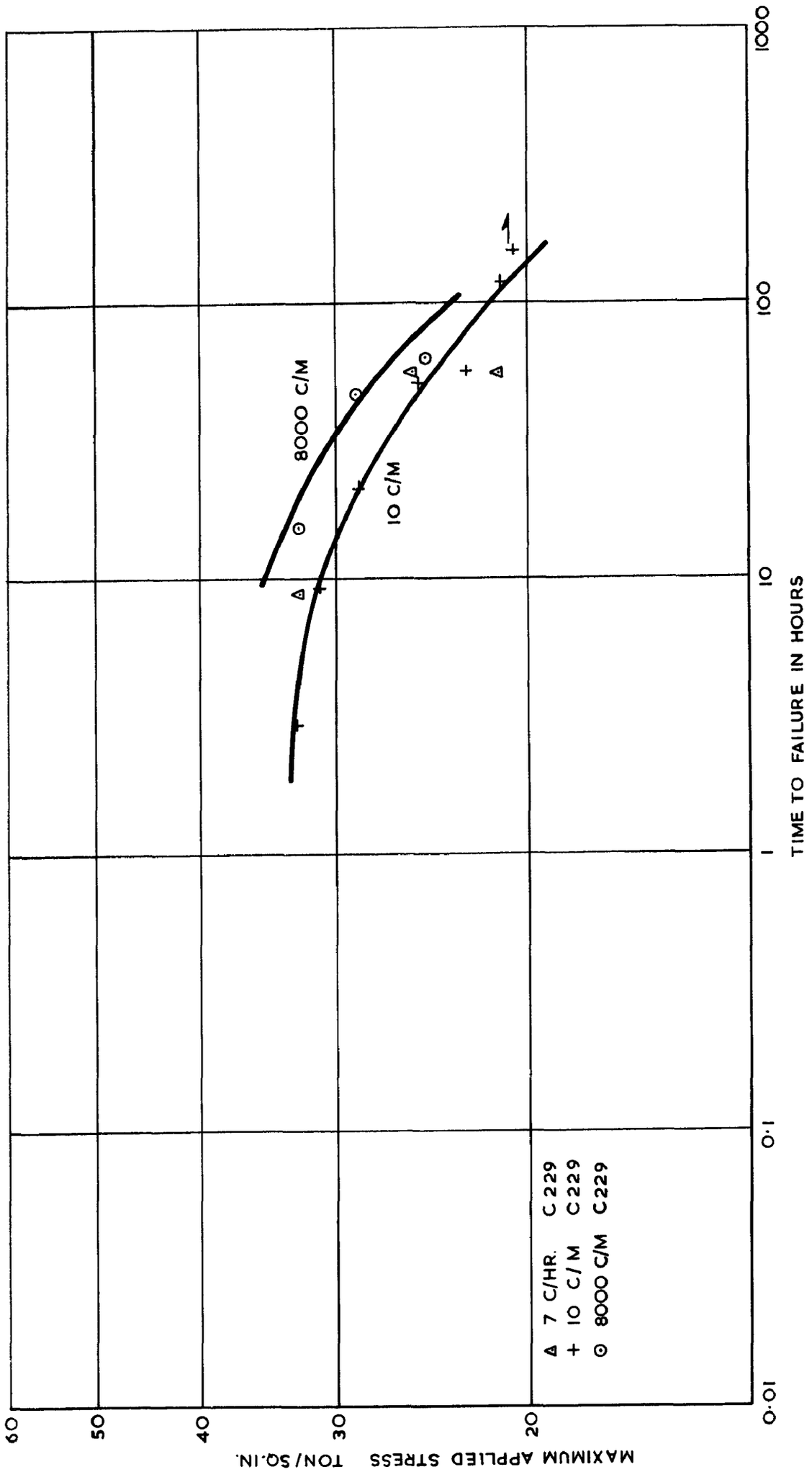

REPEAT TENSILE AT 800°C

FIG. 8.

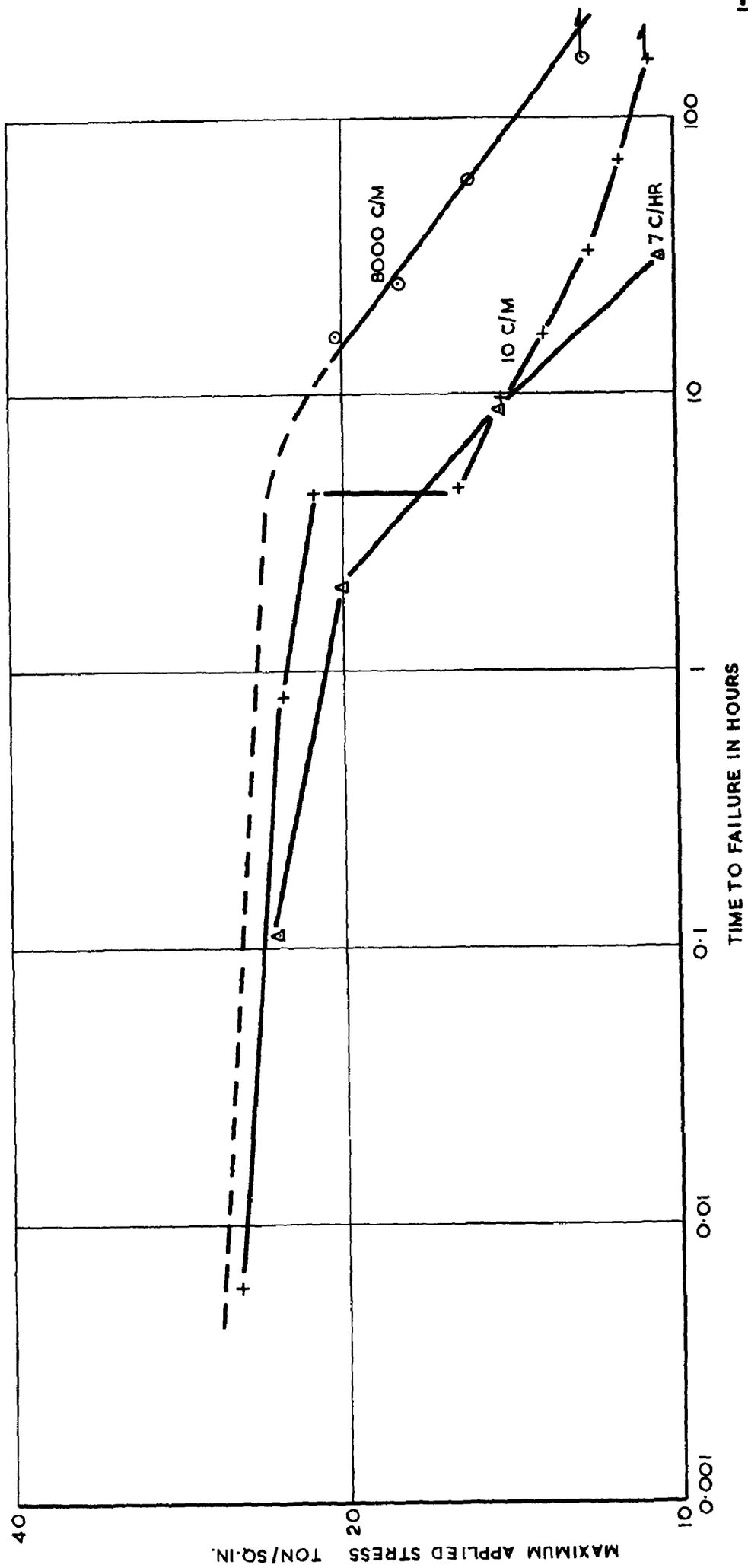

REPEAT TENSILE AT 900° C

PUSH/PULL AT ROOM TEMPERATURE

FIG. 9.

PUSH/PULL AT 600°C

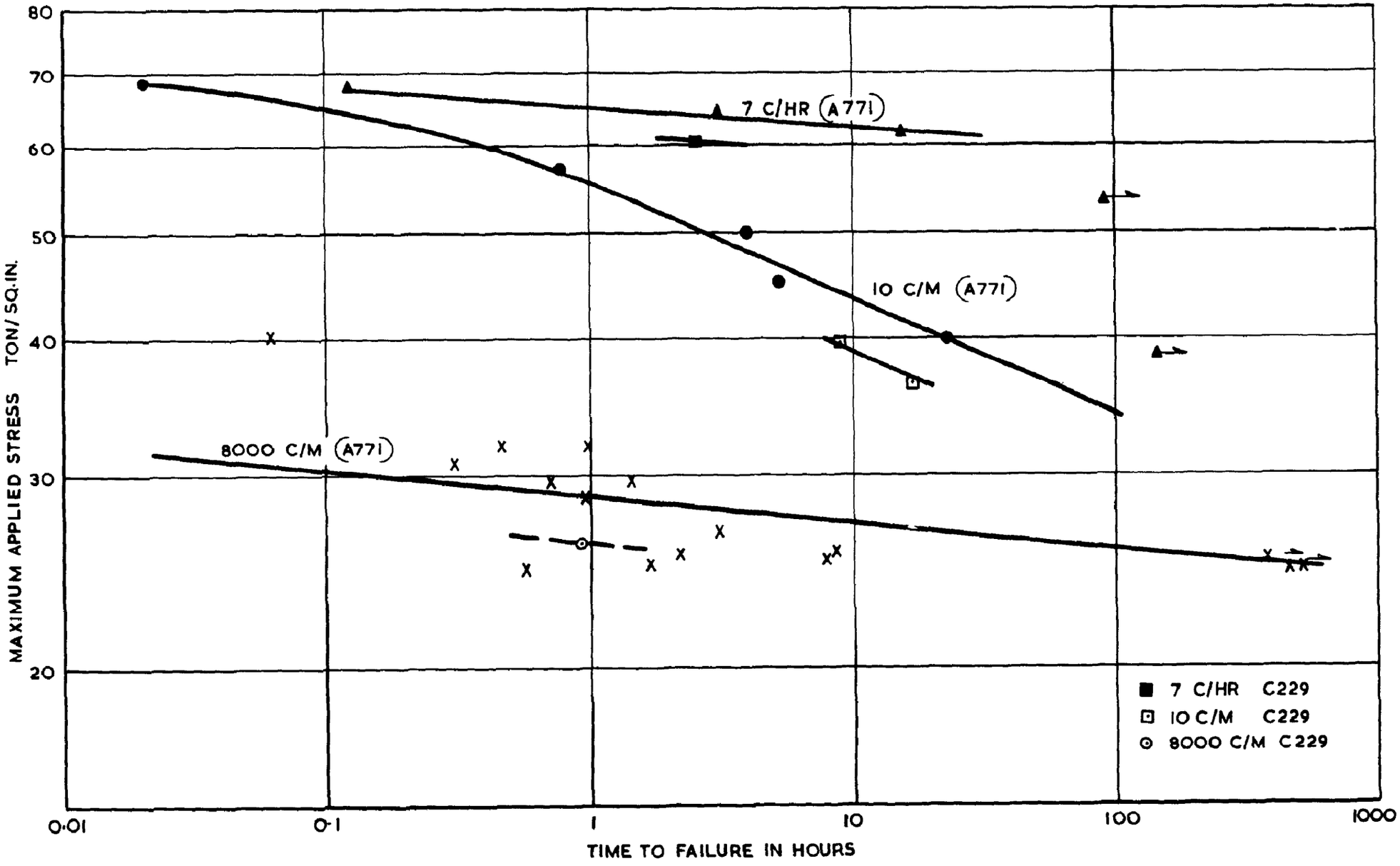

FIG.10.

PUSH/PULL AT 700° C

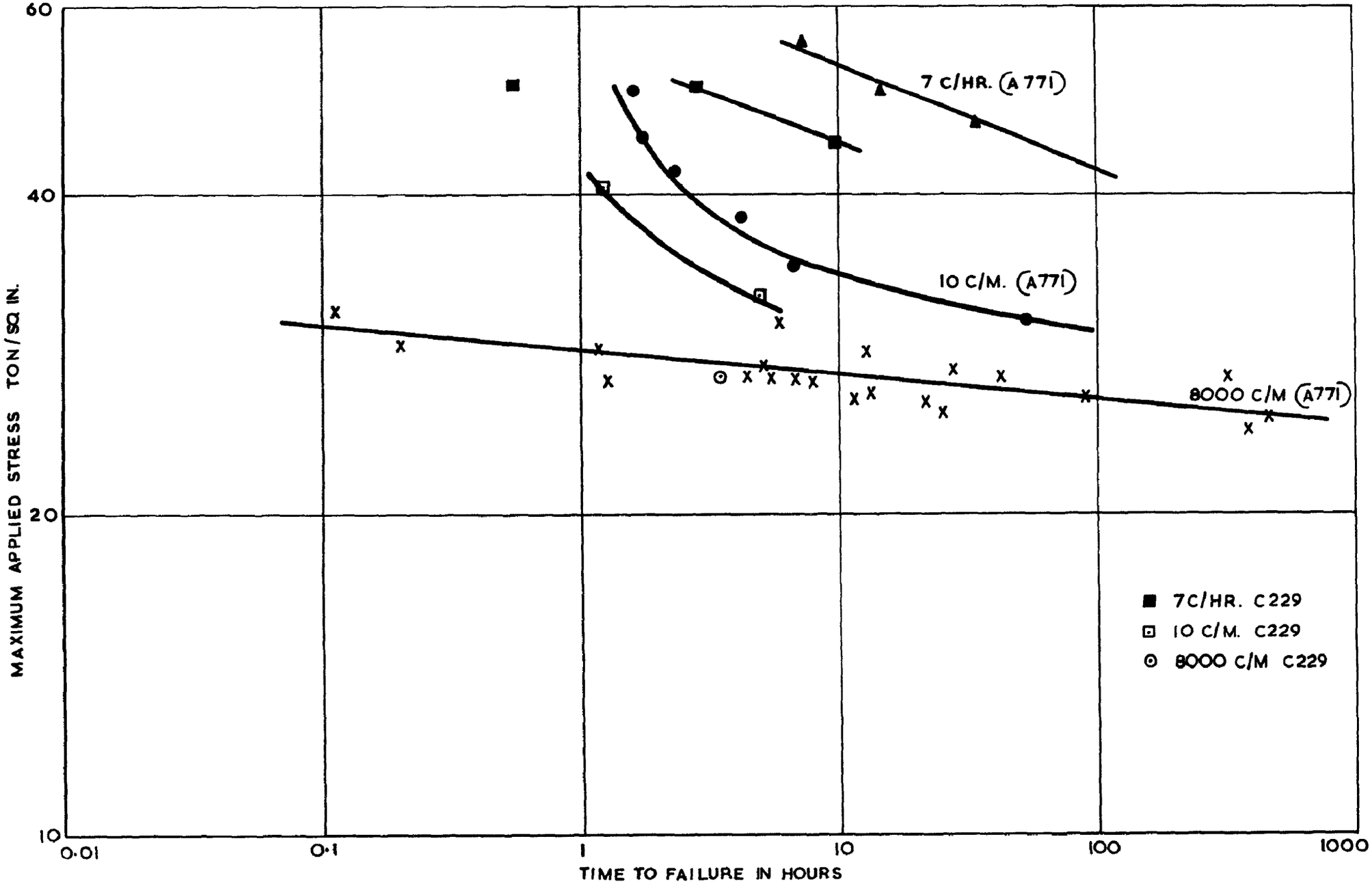

FIG. 11.

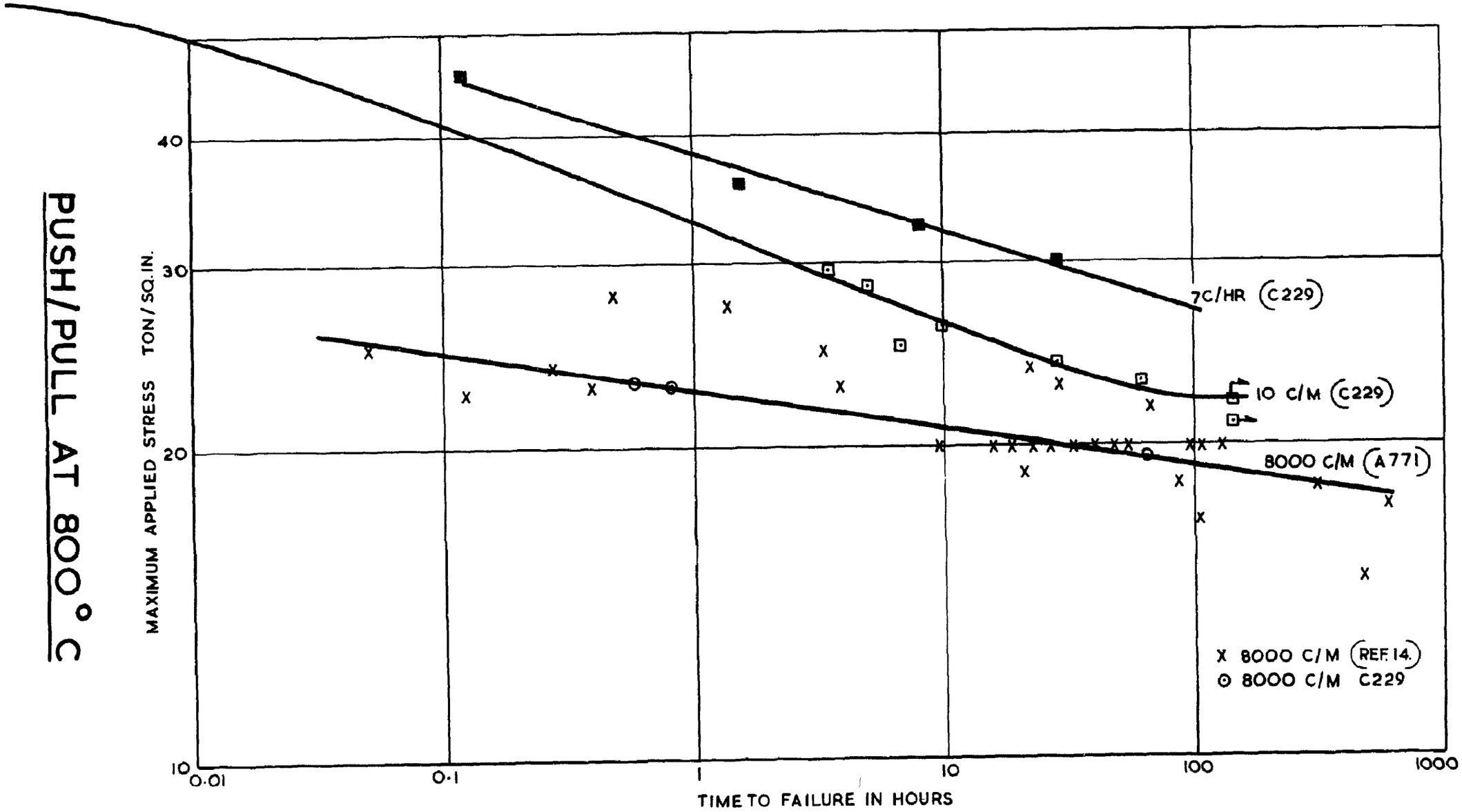
PUSH/PULL AT 800°C
MAXIMUM APPLIED STRESS TON/SQ.IN.
40
30
20
10
0.01
0·1
1
10
100
1000
TIME TO FAILURE IN HOURS
7C/HR (C229)
10 C/M (C229)
8000 C/M (A771)
X 8000 C/M (REF. 14.)
⊙ 8000 C/M C229

FIG. 12.

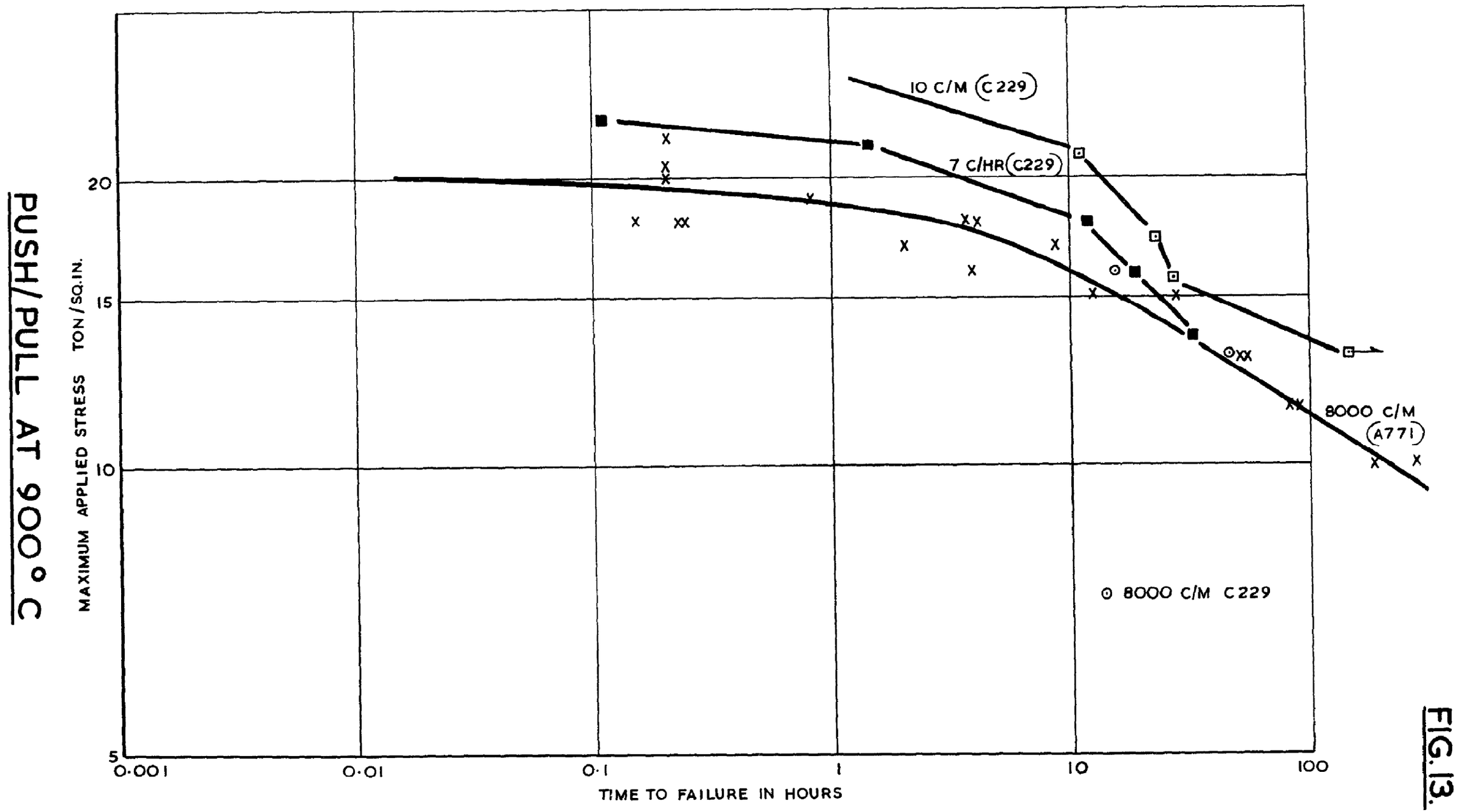
PUSH/PULL AT 900° C
MAXIMUM APPLIED STRESS TON/SQ.IN.
20
15
10
5
0·001
0·01
0·1
1
10
100
TIME TO FAILURE IN HOURS
10 C/M (C229)
7 C/HR (C229)
8000 C/M (A771)
⊙ 8000 C/M C229

FIG. 13.

FIG.14.

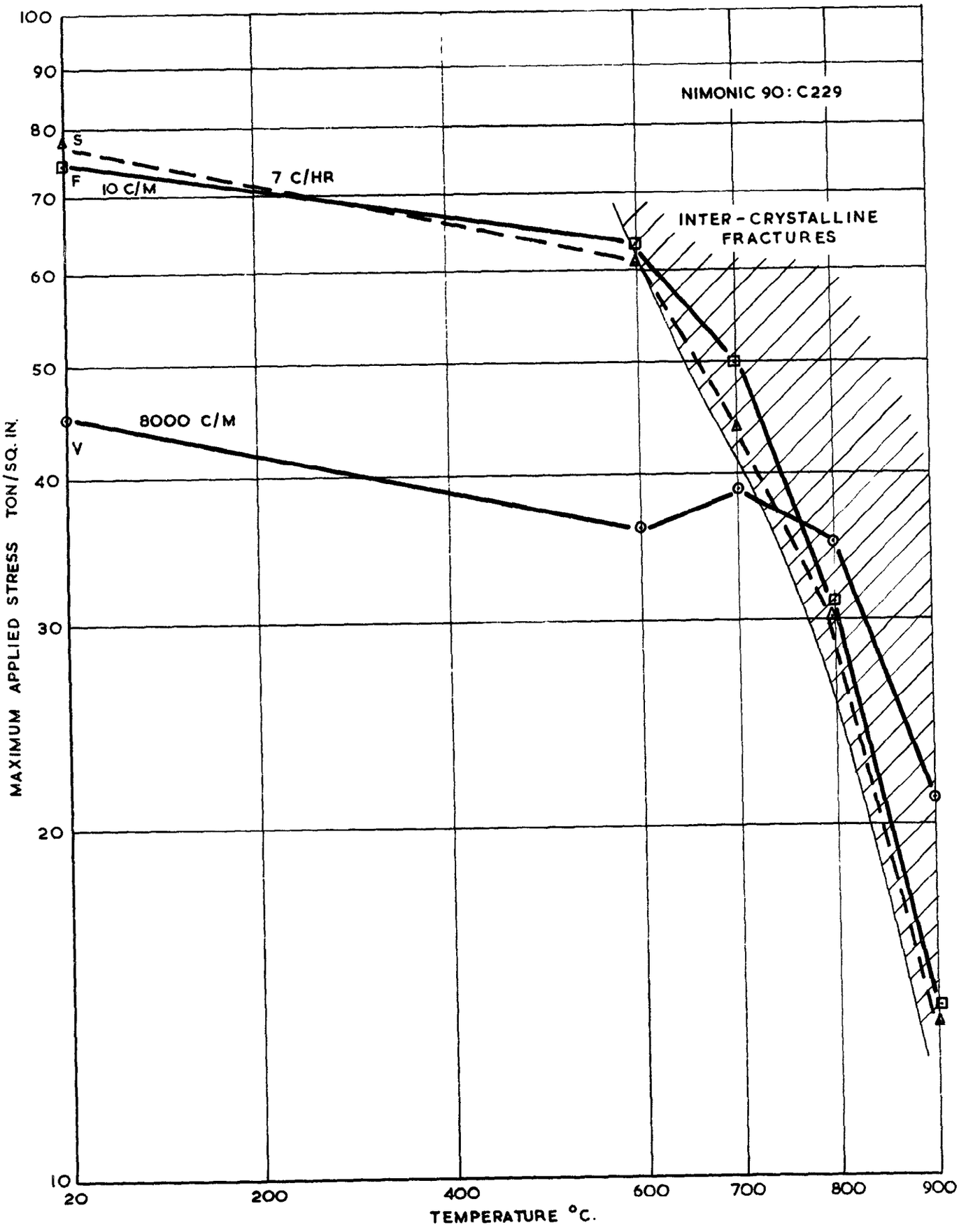

10 HOUR CROSS-PLOTS : REPEAT TENSION

FIG. 15.

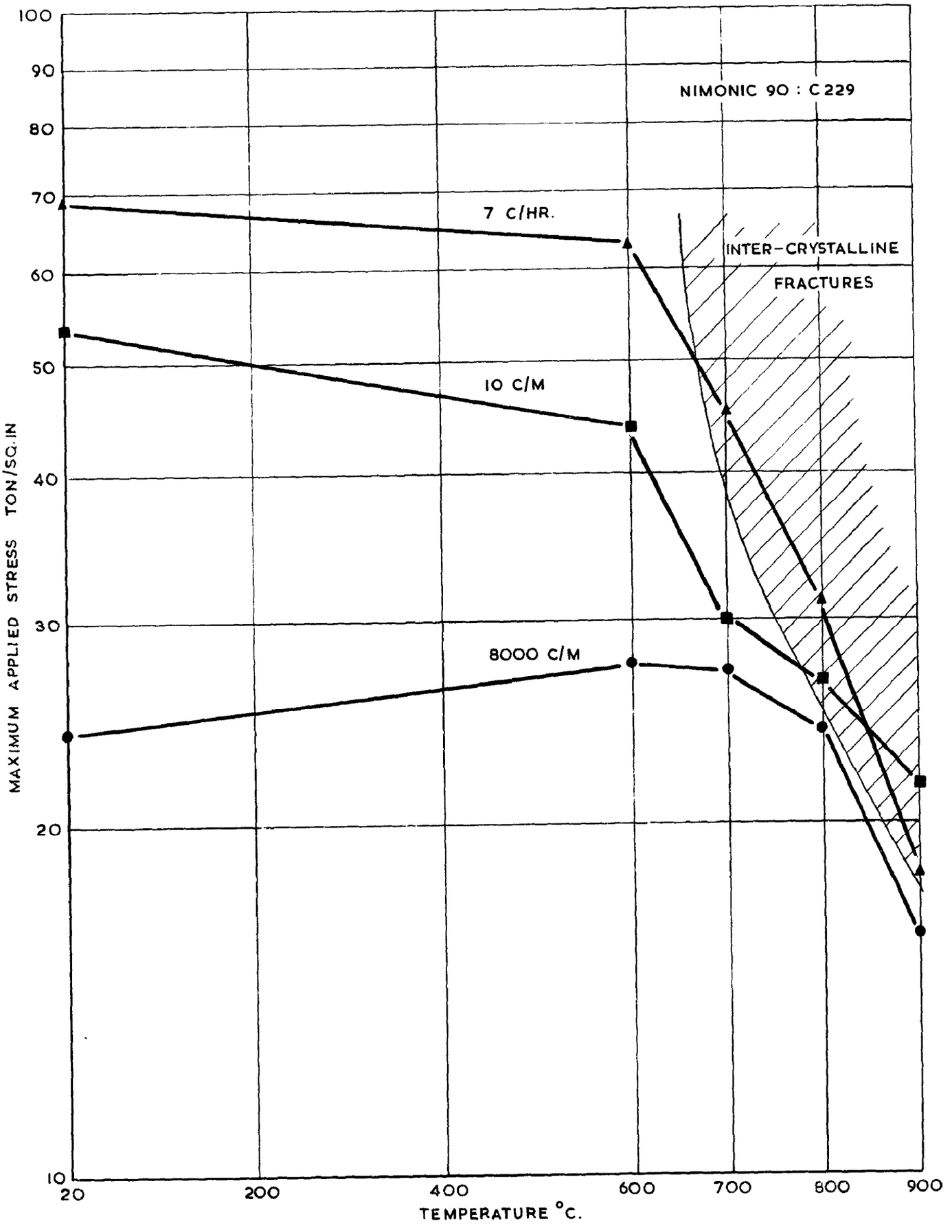

10 HOUR CROSS-PLOTS : PUSH/PULL

FIG. 16.

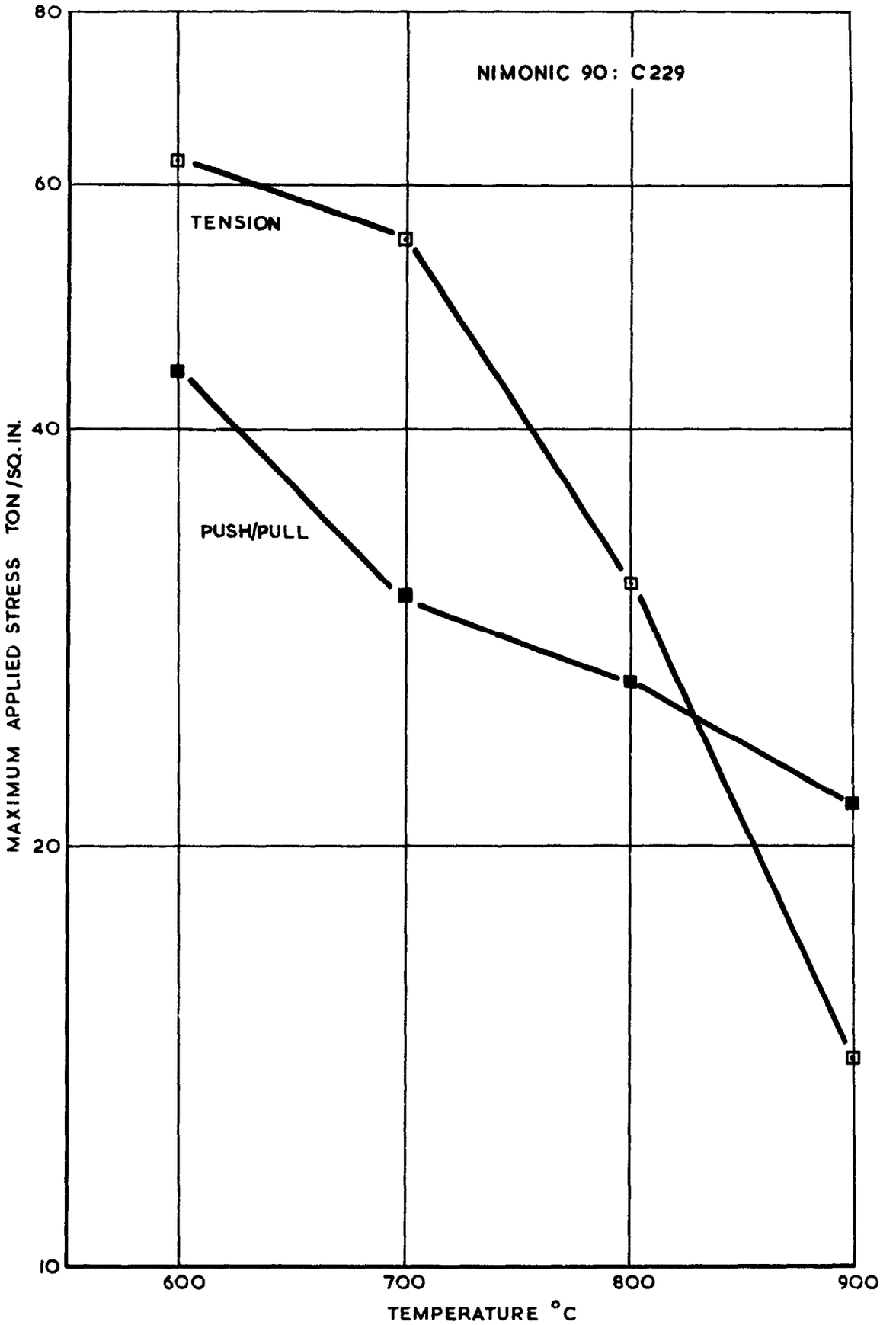

10 HOUR CROSS-PLOTS

PUSH/PULL AND TENSION AT 10 C/M

FIG.17.

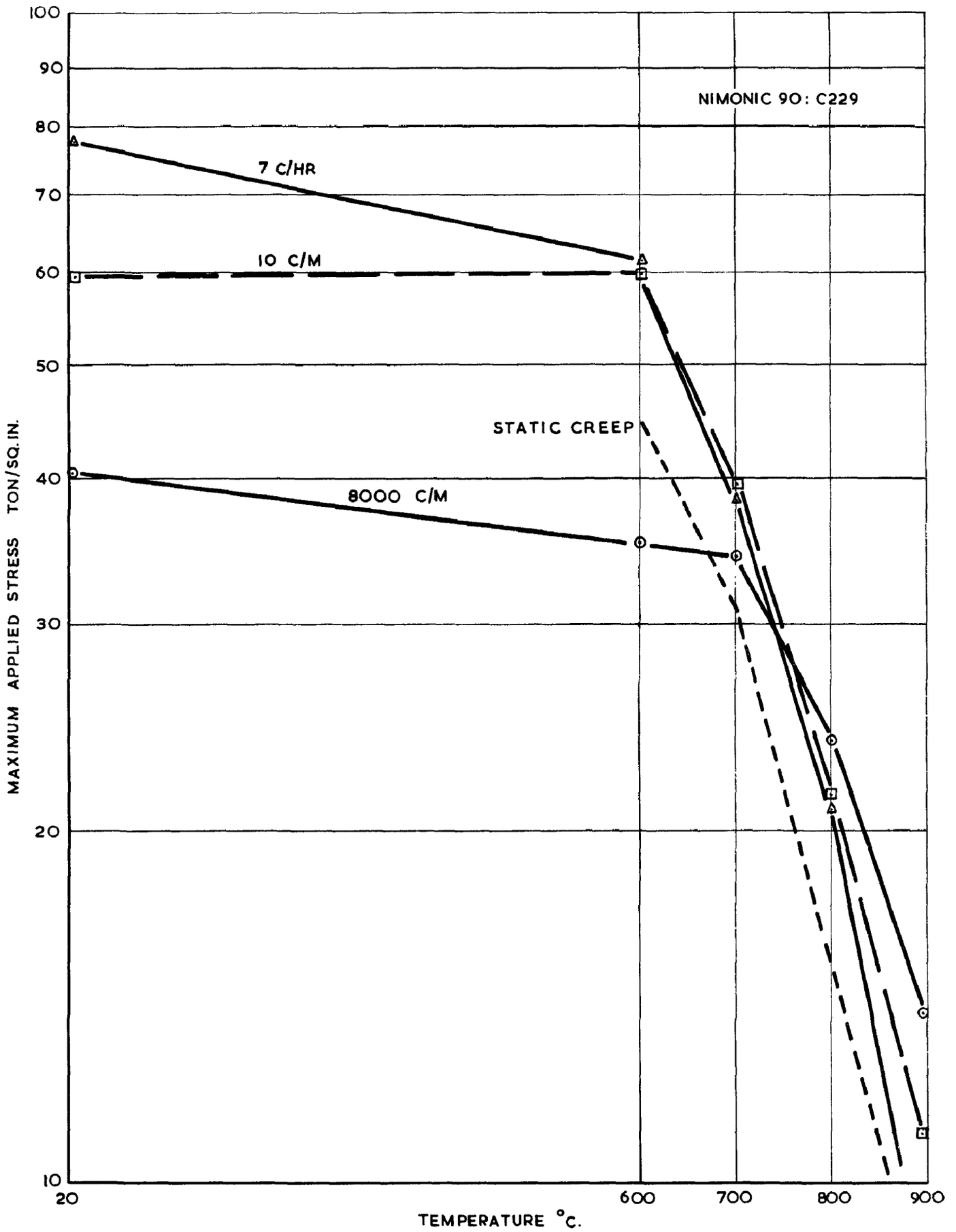

100 HOUR CROSS-PLOTS : REPEAT TENSION

FIG. 18.

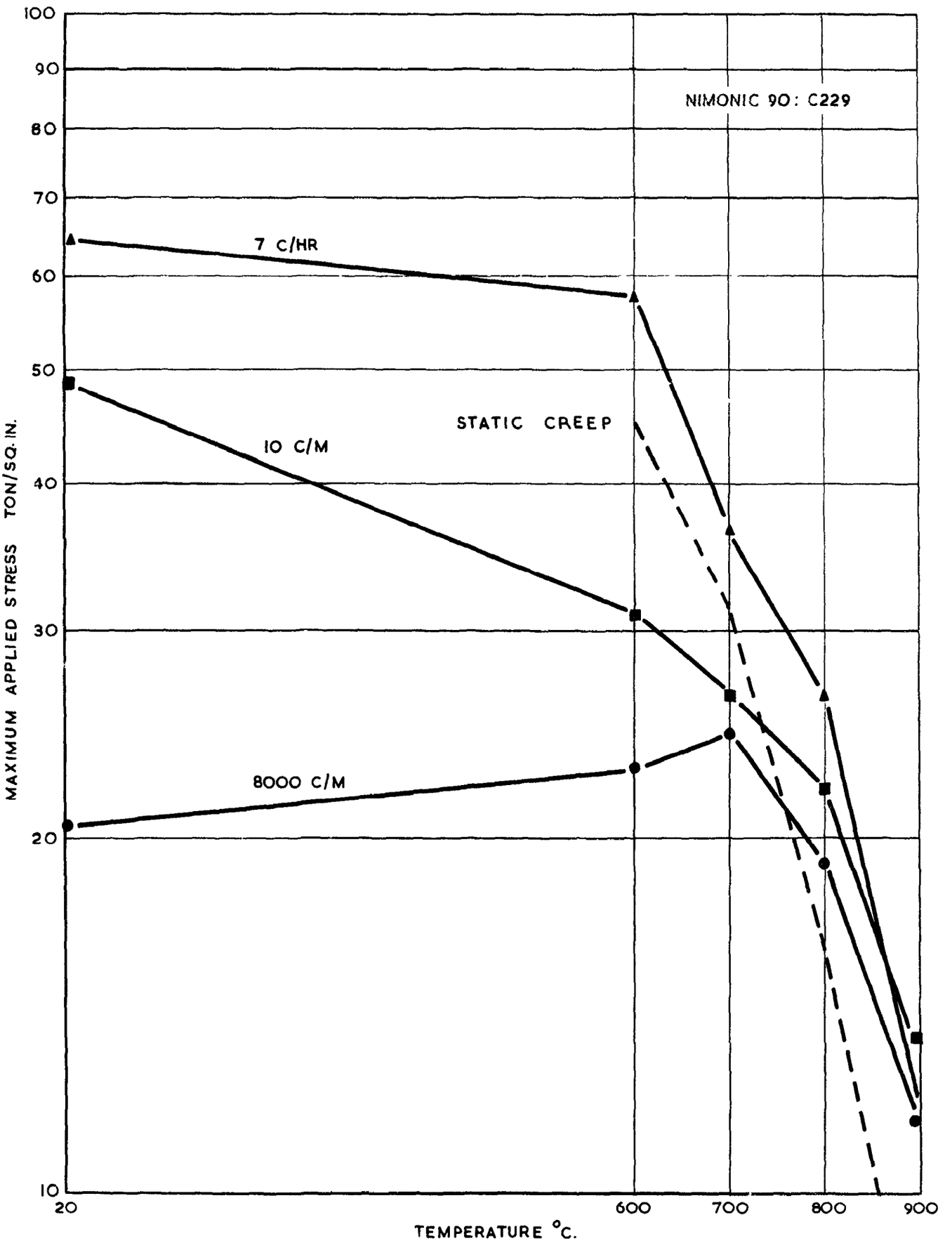

100 HOUR CROSS-PLOTS : PUSH/PULL

FIG. 19.

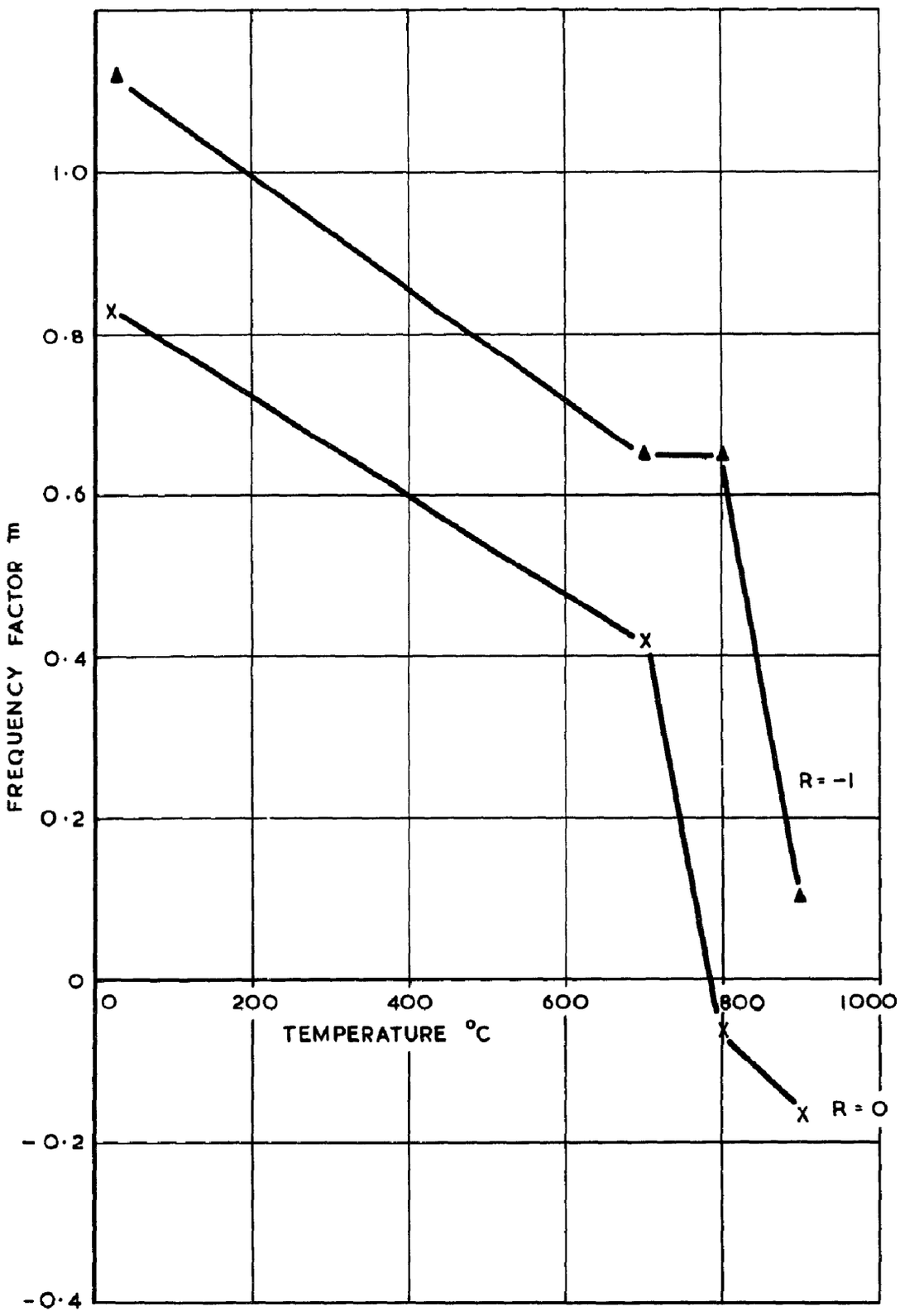

VARIATION OF THE FREQUENCY FACTOR m WITH TEMPERATURE

FIG.20.

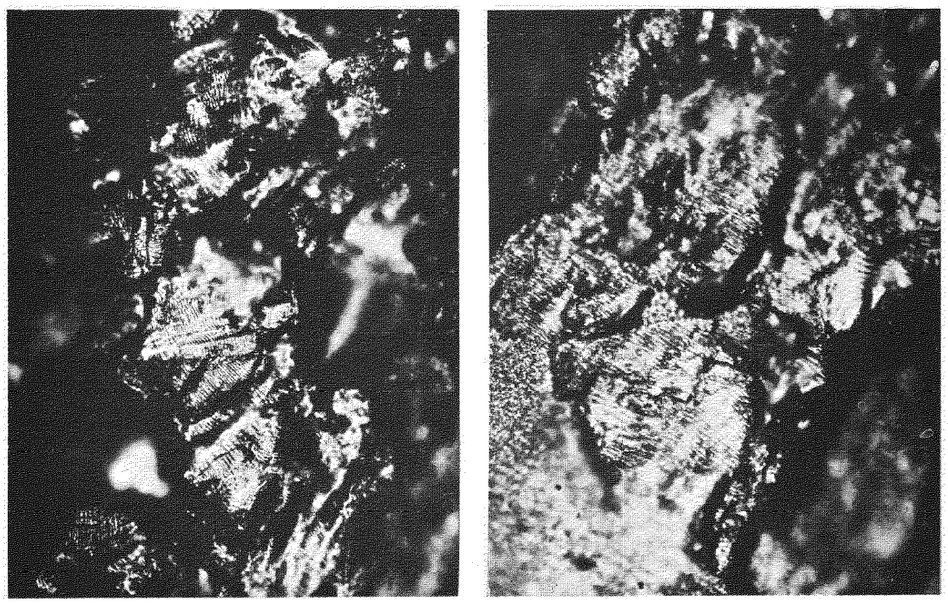

ROOM TEMPERATURE

$+42{\cdot}2$ ton/sq.in. -0

21831×10^3 cycles, 69·5 hours (A771)

700°C

$\pm 26{\cdot}9$ ton/sq.in.

1525×10^3 cycles, 3·7 hours (C 229) X400

20·1 TYPICAL STRIATIONS OBSERVED ON FATIGUE FRACTURE FACETS OF NIMONIC 90.

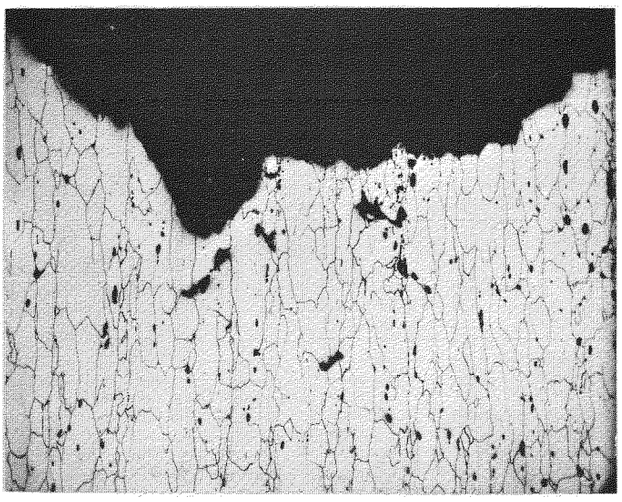

X400

600°C $+64{\cdot}9$ ton/sq.in, 0·4 hours, 210 cycles (A771) -0

20·2 TYPICAL TRANSCRYSTALLINE FRACTURE

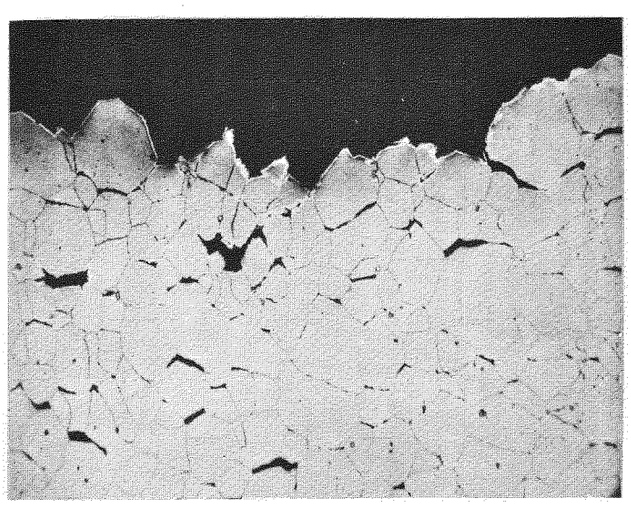

X400

900°C $+10{\cdot}4$ ton/sq.in, 31·8 hours, 320 cycles (C229) -0

20·3 TYPICAL INTERCRYSTALLINE FRACTURE

A.R.C. C.P. No. 786 539.431:669.245
December, 1963
Tilly, G. P.

EFFECTS OF VARIED LOADING PATHS ON FATIGUE ENDURANCES

PART I - SOME LOAD FATIGUE PROPERTIES OF NIMONIC 90 AT ELEVATED TEMPERATURES

The load fatigue properties of Nimonic 90 have been examined over the nominal speed range of 7 c/hr to 8000 c/min at temperatures between 20°C and 900°C under repeated tension and push/pull test conditions.

It was shown that an increase in test frequency resulted in longer lives to failure at the higher temperatures. Push/pull loading was more severe than repeated tension loading at low temperatures, but became less severe at the higher temperature. An increase in testing temperature increased the incidence of intercrystalline failure whilst increase in test frequency decreased it.

A.R.C. C.P. No. 786 539.431:669.245
December, 1963
Tilly, G. P.

EFFECTS OF VARIED LOADING PATHS ON FATIGUE ENDURANCES

PART I - SOME LOAD FATIGUE PROPERTIES OF NIMONIC 90 AT ELEVATED TEMPERATURES

The load fatigue properties of Nimonic 90 have been examined over the nominal speed range of 7 c/hr to 8000 c/min at temperatures between 20°C and 900° C under repeated tension and push/pull test conditions.

It was shown that an increase in test frequency resulted in longer lives to failure at the higher temperatures. Push/pull loading was more severe than repeated tension loading at low temperatures, but became less severe at the higher temperature. An increase in testing temperature increased the incidence of intercrystalline failure whilst increase in test frequency decreased it.

A.R.C. C.P. No. 786 539.431:669.245
December, 1963
Tilly, G. P.

EFFECTS OF VARIED LOADING PATHS ON FATIGUE ENDURANCES

PART I - SOME LOAD FATIGUE PROPERTIES OF NIMONIC 90 AT ELEVATED TEMPERATURES

The load fatigue properties of Nimonic 90 have been examined over the nominal speed range of 7 c/hr to 8000 c/min at temperatures between 20°C and 900°C under repeated tension and push/pull test conditions.

It was shown that an increase in test frequency resulted in longer lives to failure at the higher temperatures. Push/pull loading was more severe than repeated tension loading at low temperatures, but became less severe at the higher temperature. An increase in testing temperature increased the incidence of intercrystalline failure whilst increase in test frequency decreased it.

Printed and published by
HER MAJESTY'S STATIONERY OFFICE

To be purchased from
York House, Kingsway, London W.C.2
423 Oxford Street, London W.1
13A Castle Street, Edinburgh 2
109 St. Mary Street, Cardiff
39 King Street, Manchester 2
50 Fairfax Street, Bristol 1
35 Smallbrook, Ringway, Birmingham 5
80 Chichester Street, Belfast 1
or through any bookseller

Printed in England

S.O. Code No. 23-9015-86